JOURNAL OF GEOPHYSICAL RESEARCH, VOL. 96, NO. C8, PAGES 14,649–14,667, AUGUST 15, 1991

Phytoplankton Pigment Patterns and Wind Forcing off Central California

MARK R. ABBOTT AND BRETT BARKSDALE

College of Oceanography, Oregon State University, Corvallis

We use a 4-year time series of high-resolution coastal zone color scanner imagery to study mesoscale variability in phytoplankton pigment (as a surrogate for biomass) distributions off central California during the spring–summer upwelling season. We use empirical orthogonal functions to decompose the time series of spatial images into its dominant modes of variability. Similarly, we analyze wind fields derived from the Fleet Numerical Oceanography Center pressure fields. The results from these analyses are used to investigate the coupling between wind forcing of the upper ocean and phytoplankton distributions on mesoscales. Prior to the spring transition, wind stress is dominated by strong northward conditions, and pigment is low and relatively uniform throughout the California Current domain. The first strong southward wind event soon results in a bloom of phytoplankton that is also uniformly distributed offshore. Nearshore values fluctuate relatively little in response to variations in wind forcing. After the spring transition, the wind becomes more steady (southward) and the fluctuations are dominated by changes in the strength of the curl. During southward events, the curl tends to become more positive. Depending on the fluctuations and strength of these curl episodes, filaments begin to form at particular locations. The overall pigment concentration in the California Current drops as a larger fraction of the pigment is distributed within the filaments. The filaments also tend to become shorter during this period, which starts soon after the spring transition and usually reaches its maximum intensity in early summer. Winds (and curl) become much weaker in the mid-July to August period, and the filaments become much less prominent in terms of concentration and their length increases. Isolated wind events occasionally reinvigorate the filaments. A final bloom in the fall occasionally appears with spatial structure similar to the spring bloom. We conclude that wind forcing, in particular the curl of the wind stress, plays an important role in the distribution of phytoplankton pigment in the California Current. Although the underlying dynamics, especially of the filaments, may be dominated by processes other than forcing by wind stress curl (such as eddies or topographically induced instabilities), it appears that curl may force the variability of the filaments and hence the pigment patterns.

INTRODUCTION

The California Current is typical of eastern boundary currents; flow patterns are complex, often dominated by mesoscale features, and primary production is high [*Wooster and Reid*, 1963; *Hickey*, 1979]. Large-scale processes have been studied in the California Current for over 40 years by the California Cooperative Oceanic Fisheries Investigations (CalCOFI). Results from CalCOFI and other studies show the California Current to be a complicated system of surface currents and undercurrents that vary considerably on seasonal and interannual time scales [*Hickey*, 1979; *Chelton*, 1984; *Huyer*, 1983; *Lynn and Simpson*, 1987]. Forcing by the alongshore wind stress and particularly the curl of the wind stress are important [*Strub et al.*, 1987; *Chelton*, 1982]. Wind stress along the northern California coast during late spring is often in excess of 1 dyn/cm^2. Forcing by remote events in the eastern tropical Pacific [*Chelton and Davis*, 1982; *Chelton et al.*, 1982] may also be important. In parallel with the large-scale observations, several intensive field programs have noted the strong mesoscale variability of the California Current. Although mesoscale eddies are not as energetic in the California Current as in western boundary currents [*Bernstein*, 1983], they play an important role in the overall dynamics of the California Current [*Simpson et al.*, 1984; *Mooers and Robinson*, 1984; *Rienecker and Mooers*, 1989]. Several recurrent eddies have been detected in the large-scale CalCOFI surveys [*Simpson et al.*, 1986; *Hickey*, 1979]. Offshore filaments are also important in the redistribution of heat, momentum, and materials [*Coastal Transition Zone Group*, 1988; *Flament et al.*, 1985; *Kosro and Huyer*, 1986; *Hood et al.*, 1990] and tend to be recurrent features near coastal promontories [*Kelly*, 1985]. The coupling between these energetic mesoscale phenomena and the large-scale biological and physical dynamics of the California Current is difficult to make using conventional ship observations, although not impossible [*Simpson et al.*, 1986].

One approach is to use long time series of high-resolution satellite data to study this mesoscale/large-scale coupling. Although there are numerous studies using short sequences of satellite data, there are some studies centered on long time series. *Kelly* [1985] used a 4-month sequence of advanced very high resolution radiometer (AVHRR) data to study sea surface temperature (SST) patterns off northern California and their relationship to wind forcing. Patterns of phytoplankton pigment were investigated off northern California using coastal zone color scanner (CZCS) imagery [*Abbott and Zion*, 1987]. *Peláez and McGowan* [1986] studied biological patterns in the California Current using selected CZCS data from 1979–1982. A 2.5-year time series of CZCS and AVHRR images was studied by *Smith et al.* [1988] and *Michaelsen et al.* [1988]. Recent work was reported by *Thomas and Strub* [1989, 1990] and *Strub et al.* [1990] on the relationship between large-scale wind forcing and phytoplankton pigment patterns using a 6-year CZCS time series. A consistent result of these studies is that the temporal and spatial patterns of phytoplankton closely parallel the patterns observed in the physical variables. Productivity in the California Current is high, although there is evidence that these high levels of production are not driven entirely by coastal upwelling but are a combination of southward transport of nutrient-rich subarctic waters and Ekman pumping driven by the curl of the wind stress [*Chelton et al.*, 1982; *Chelton*, 1982; *Smith et al.*, 1988; *Strub et al.*, 1990; *Thomas and Strub*, 1990].

Paper number 91JC01207.
0148-0227/91/91JC-01207$05.00

One of the key questions concerning the dynamics of the California Current is the nature of the forcing mechanisms associated with the large-scale filaments or meanders [*Coastal Transition Zone Group*, 1988; *Strub et al.*, this issue]. Considerable evidence suggests that dynamic instabilities resulting from either topographic interactions or baroclinic processes are dominant [e.g., *Willmott*, 1984; *Ikeda and Emery*, 1984]. However, *Kelly* [1985] suggests that there is a close coupling with spatial and temporal variations in the wind field. Numerous models appear to be able to generate "reasonable" filaments [e.g., *Haidvogel et al.*, this issue] that resemble those observed in field and satellite data. The question still remains as to whether the dynamics are correct or the statistics of the simulated features are accurate.

In this paper, we use a 4-year time series of high-resolution CZCS imagery to study mesoscale variability in phytoplankton pigment (as a surrogate for biomass) distributions off central California during the spring–summer upwelling season [*Huyer*, 1983]. We use empirical orthogonal functions (EOF) to decompose the time series of spatial images into its dominant modes of variability. Similarly, we analyze wind fields derived from the Fleet Numerical Oceanography Center (FNOC) pressure fields. The results from these analyses are used to investigate the coupling between wind forcing of the upper ocean and phytoplankton distributions on mesoscales.

METHODS

Processed CZCS data were obtained from the West Coast Time Series project. The CZCS data that were used cover the March–October period (the primary upwelling season) from the years 1980–1983 and the region from 30°N to 40°N and 230°E to 240°E (120°W to 130°W) (Figure 1). The data were processed using software developed at the University of Miami by O. Brown and R. Evans, based on algorithms developed by *Gordon et al.* [1983*a*, *b*]. Atmospheric correction was based on a single-scattering Rayleigh correction [*Gordon and Castaño*, 1987; *Gordon et al.*, 1988*a*] and a fixed set of epsilons for aerosol correction [*Feldman at al.*, 1989]. The data were remapped to a fixed grid where each pixel had a resolution of 0.01° (nominally 1 km). A complete description of the processing methods and possible sources of errors in the data set are described in the Appendix of *Strub et al.* [1990].

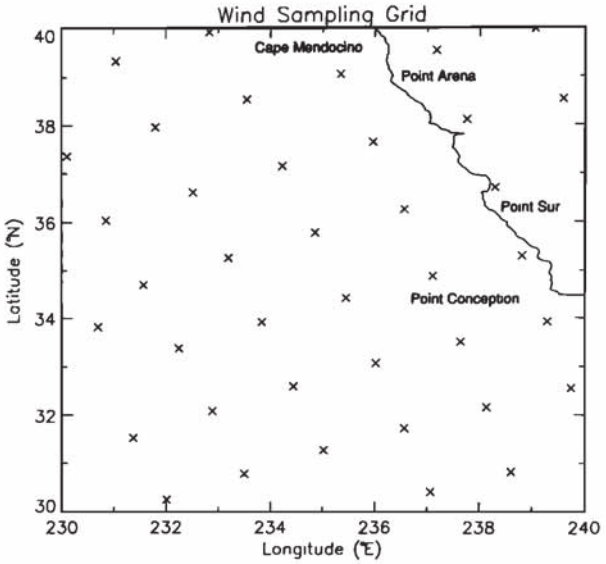

Fig. 1. Sample locations for wind stress field.

After conversion of the raw data into gridded maps of phytoplankton pigment, an image of 506 by 506 pixels was created with a spatial resolution of 2.2 km. Initially, 224 images were screened for analysis. Some images were discarded, as they contained little usable data in the study domain or were at the edge of the CZCS swath. Because of the tendency of clear images to be "clumped" together in time [*Abbott and Zion*, 1987; *Kelly*, 1985; *Michaelsen et al.*, 1988; *Chelton and Schlax*, this issue], we formed temporal and spatial averages of these images. We estimated the correlation scale to be approximately 12 km in the east-west direction and 8 km in the north-south direction for a 3-day averaging period. That is, features larger than these scales were reasonably uncorrelated with adjacent features. The 3-day averaging period was also selected as the decorrelation scale [*Kelly*, 1985; *Denman and Abbott*, 1988]. This reduces the dominance of individual cloud-free periods in the analysis. As more images were collected in 1980 and 1981 than in the other 2 years, we derived a mask based on 1980–1981 coverage. If a given pixel was not cloud-free at least 50% of the time, it was masked. This mask was used for all 4 years. Some pixels were included that would not have met the 50% criterion if we had considered the complete, 4-year time series. However, this was a relatively small proportion of the total series and did not significantly affect the final mask. This final, reduced-resolution data set had 46 realizations in 1980, 49 in 1981, 33 in 1982, and 21 in 1983. This decrease in sampling over the 4-year period was largely a function of CZCS mission operations and data collection, rather than a function of cloudiness.

The CZCS algorithms produce images of $\log_{10}$ (pigment); we left the data in this form because pigment is log normally distributed in this region, as are many biological properties [*Denman and Abbott*, 1988; *Roesler and Chelton*, 1987]. This essentially "filters" out isolated events. However, the CZCS time series does not resolve such events adequately so we feel that this is not a serious drawback in our analysis.

The individual images were arranged as data vectors and combined to form a single matrix where each column of the matrix corresponded to a single time-averaged image [*Kelly*, 1985; *Eslinger et al.*, 1989]. There were 6079 spatial locations for each image. Rather than construct the covariance matrix, we employed singular value decomposition (SVD) in the same manner as *Kelly* [1985] to yield the first N eigenvalues and eigenvectors where N is the number of time samples. This was done after first removing the temporal mean from each image. The SVD method requires that the data set be complete with no spatial gaps. This condition is not met with this data set, so missing data were filled in with the temporal average for that particular location. As we have initially eliminated any locations that are observed less than 50% of the time, this crude method of gap filling should not obscure the general patterns of the lower order EOFs.

Comparisons with ship data have shown the satellite estimates to be within a factor of 2 for most regions [*Gordon et al.*, 1983*a*; *Balch et al.*, 1989; *Denman and Abbott*, 1988; *Smith et al.*, 1988]. There are several sources of algorithm error that may affect any statistical analysis. These are described in detail by *Strub et al.* [1990] and include incorrect cloud masking and "ringing," incorrect aerosol removal, sensor degradation, incorrect Rayleigh scattering estimates, and interference by nonchlorophyll materials. We briefly review the potential contributions of each error source to our analysis. Pixels that are contaminated by clouds or are affected by ringing [*Mueller*, 1988; *Eckstein and Simpson*, 1991*a*] may be included in the analysis by using a fixed threshold. As cloud patterns have short decorrelation time scales, this will not be a significant problem in the averaged time series. Also, the

mesoscale patterns should not be significantly affected in the EOF analysis. Aerosol removal may be a problem if the type of aerosol changes significantly within an image [*Eckstein and Simpson*, 1991*b*]. However, this should not be a significant problem off the U. S. west coast, where the prevailing winds will transport marine aerosols into the study region. As with the cloud masking, these effects should have short temporal scales and thus should not significantly affect the EOF analysis of the smoothed series.

Degradation of the CZCS has been the focus of much research [*Gordon et al.*, 1983*b*; *Mueller*, 1985]; an understanding of this decay in radiometric sensitivity is essential for studies of long CZCS time series. Present work suggests that the decay of the CZCS was relatively stable through 1981 and then became more complicated until the demise of the sensor in 1986 (R. Evans, personal communication, 1989). As the degradation of the sensor was not a smooth process but rather occurred as a series of discrete jumps, this will introduce another potential source of small-scale temporal variability in the time series. It may also affect the interpretation of long-time-scale changes. The small-scale changes should have limited influence on the EOF analysis as the data are first smoothed. The long-term changes in the CZCS will be more difficult to remove, although this effect should be manifested in changes in the mean fields rather than as changes in the fields of spatial variability. That is, the EOF modes should not be affected, although interannual changes in the amplitudes may be affected by sensor decay.

Under conditions of large solar angles (e.g., winter at high latitudes), CZCS estimates of pigment appear to be erroneously high because of incorrect Rayleigh correction [*Strub et al.*, 1990; *Gordon et al.*, 1988*a*]. Use of a multiple scattering Rayleigh model should reduce this problem [*Gordon and Castaño*, 1987; *Gordon et al.*, 1988*b*; *Strub et al.*, 1990; *Feldman et al.*, 1989]. However, this should not be a significant problem in our analysis, as we are working with data south of 40°N between March and October where solar angles will not be excessively large.

The final source of error is interference by nonpigment materials. This will be important in areas of high terrigenous input such as San Francisco Bay as well as areas of high dissolved organic material (DOM) concentrations. The effects of terrigenous input will be localized near the coast and should not pose a problem for the analysis. The effects of DOM are not as well understood. *Peacock et al.* [1988] noted high gelbstoffe concentrations at the seaward ends of the large coastal filaments, presumably the result of zooplankton grazing. DOM levels were high enough such that the usual CZCS algorithms would not estimate phytoplankton pigment concentrations properly [*Carder et al.*, 1989]. As this phenomenon has not been systematically studied in the California Current, we cannot quantify its potential effects on the EOF analysis. If DOM originates as a result of zooplankton grazing, we expect it to be quite patchy in time and space. Thus if DOM concentrations are high in some areas, they may have an impact on the patterns of variability estimated by EOF analysis.

Despite these potential sources of error in the CZCS time series, the most serious problem will be gaps in the data set [*Strub et al.*, 1990; *Chelton and Schlax*, this issue]. As the gaps are largely caused by clouds, which are closely related to the wind patterns [*Michaelsen et al.*, 1988; *Abbott and Zion*, 1987; *Simon*, 1977; *Beardsley et al.*, 1987], the CZCS data set will be biased. For example, a CZCS time series from off northern California was generally cloudy when alongshore wind speeds were < 9 m/s [*Abbott and Zion*, 1987]. *Michaelsen et al.* [1988] found a similar bias, although cloudy conditions were generally associated with high wind speeds. In general, the patterns of wind forcing (and hence cloud patterns) have time scales of 4–6 days associated with synoptic-scale atmospheric disturbances [*Simon*, 1977; *Beardsley et al.*, 1987]. Thus we have attempted to reduce the effects of this wind bias by averaging over 3 days, similar to *Kelly* [1985]. Other gaps arise because of the orbit characteristics of the satellite as well as operations of the sensor and the data collection system. As noted earlier, coverage in 1982 and 1983 was significantly less than during prior years. The results from these 2 years should be used for qualitative comparisons only.

The wind fields were produced from pressure fields by FNOC every 12 hours and have been described by *Strub and James* [1990], who provide comparisons between the FNOC fields and buoy and ship observations. The standard FNOC grid has a resolution of approximately 380 km. These winds were interpolated to the Limited-Area Fine Mesh (LFM) model grid (with a resolution of about 190 km) from the National Meteorological Center. The FNOC surface wind fields were converted to wind stress using a variable drag coefficient following *Large and Pond* [1981]. The wind stress fields were relatively smooth [*Strub and James*, 1990], reflecting their origin from pressure fields. They do not resolve the small-scale patterns of variability. *Strub and James* [1990] report a comparison of the LFM and FNOC winds. They note that the FNOC winds reproduced the patterns of curl more accurately than the LFM winds. We analyzed both sets and chose to present the FNOC winds; there was little difference between the two sets except for the intensity of the curl which was generally stronger in the FNOC fields even though they were derived from an interpolated field.

Strub and James [1990] report a comparison of the LFM and FNOC winds. They note that the FNOC winds reproduced the patterns of curl more accurately than the LFM winds. We analyzed both sets and chose to present the FNOC winds; there was little difference between the two sets except for the intensity of the curl, which was generally stronger in the FNOC fields even though they were derived from an interpolated field.

After conversion to wind stress, 3-day vector averages of the wind stress fields were calculated. We used the varimax method for rotating the wind stress EOFs [*Preisendorfer*, 1988; *Richman*, 1981]. The varimax rotations are particularly useful for data sets where the anomalies tend to cluster in isolated groups, such as often occur with wind observations [*Richman*, 1981] where there are preferred directions. The varimax rotation often results in more understandable patterns, although the amplitude time series are no longer uncorrelated. There were 39 spatial locations with interpolated wind stress data that corresponded to the sample region (Figure 1). The resulting covariance matrix could be handled straightforwardly without resorting to SVD methods.

RESULTS

The temporal means for each year are shown in Plate 1. (Plates 1 and 2 are shown here in black and white. The color versions can be found in the separate color section in this issue.) Patterns of mean pigment from 1980 and 1981 (Plates 1*a* and 1*b*) look similar; there is a broad band of fairly high pigment (>1.0 mg/m^3) extending ~300 km offshore. The offshore edge of this band is clearly scalloped, although this pattern is more distinct in 1981. The high-pigment band extends farther offshore in the northern part of the domain during 1980 than in 1981. Nearshore, there is a narrow band (~50 km) of higher pigment along the entire coastline, especially from Monterey Bay to Point Arena. In 1982 (Plate 1*c*), the general patterns are the same although the band

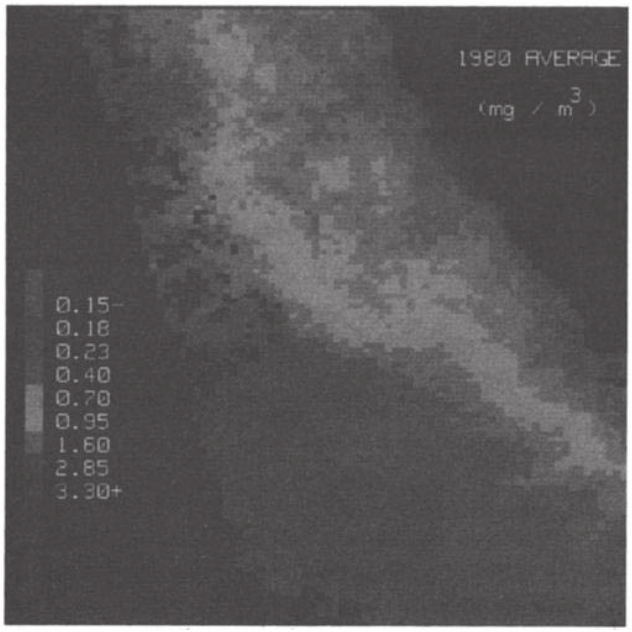

Plate 1*a*

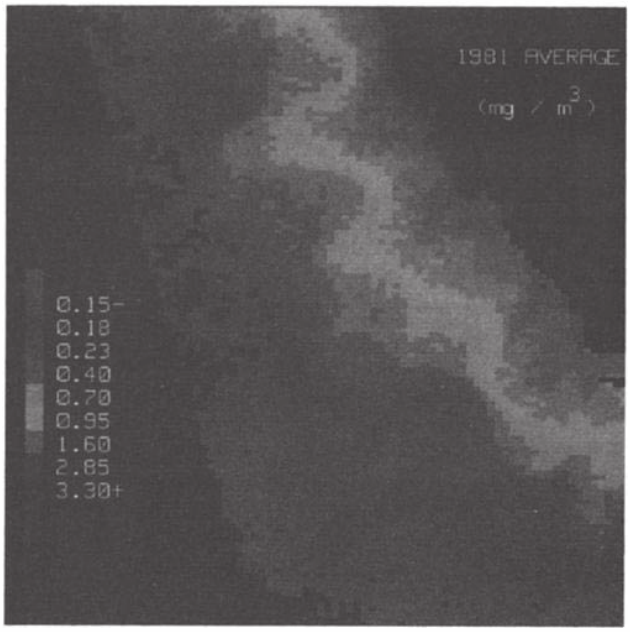

Plate 1*b*

Plate 1*c*

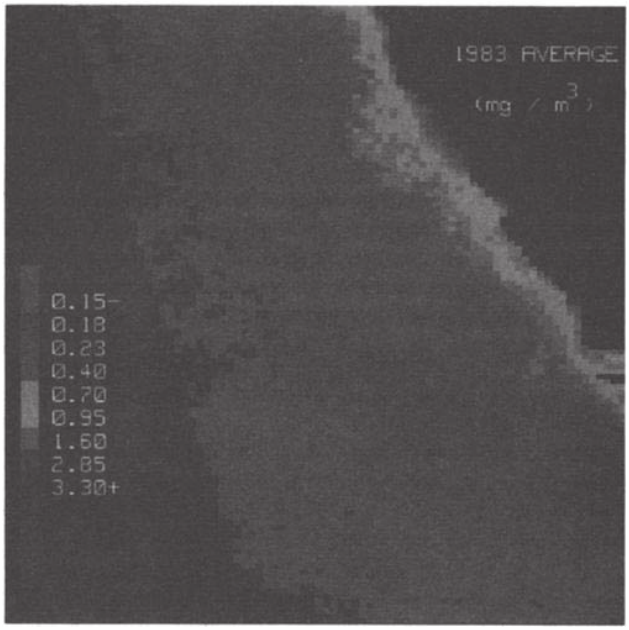

Plate 1*d*

Plate 1. (*a*) Mean of CZCS-derived pigment images for the period March–October 1980. (*b*) Same as in Plate 1*a* but for 1981. (*c*) Same as in Plate 1*a* but for 1982. (*d*) Same as in Plate 1*a* but for 1983. (*e*) Same as in Plate 1*a* but for all 4 years. (The color version of this figure can be found in the separate color section in this issue.)

is much more variable offshore. The area of high pigment is generally narrower than in 1981. The mean pattern from 1983 (Plate 1*d*) is considerably different, with no evidence of a broad offshore band of high pigment and only a narrow, nearshore band of high pigment. This pattern is consistent with the 1982–1983 El Niño which apparently displaced biological patterns northward [*Pearcy and Schoener*, 1987; *Strub et al.*, 1990]. The absence of offshore high-pigment water in 1983 was observed by *Fiedler* [1984] and *Strub et al.* [1990]. The mean for the entire series (Plate 1*e*) has scallops off Cape Mendocino, Point Arena, and Point Sur as in 1981, though they are less pronounced.

We used the complete 4-year time series for the EOF analysis. For comparison, we also used each year separately to study the interannual differences in detail. Plate 2*a* shows the first mode which accounts for 30.4% of the variance. The large region of strongly negative coefficients is roughly coincident with the core of the California Current [e.g., *Hickey*, 1979; *Chelton*, 1982; *Lynn and Simpson*, 1987]. There is a narrow band of small, negative

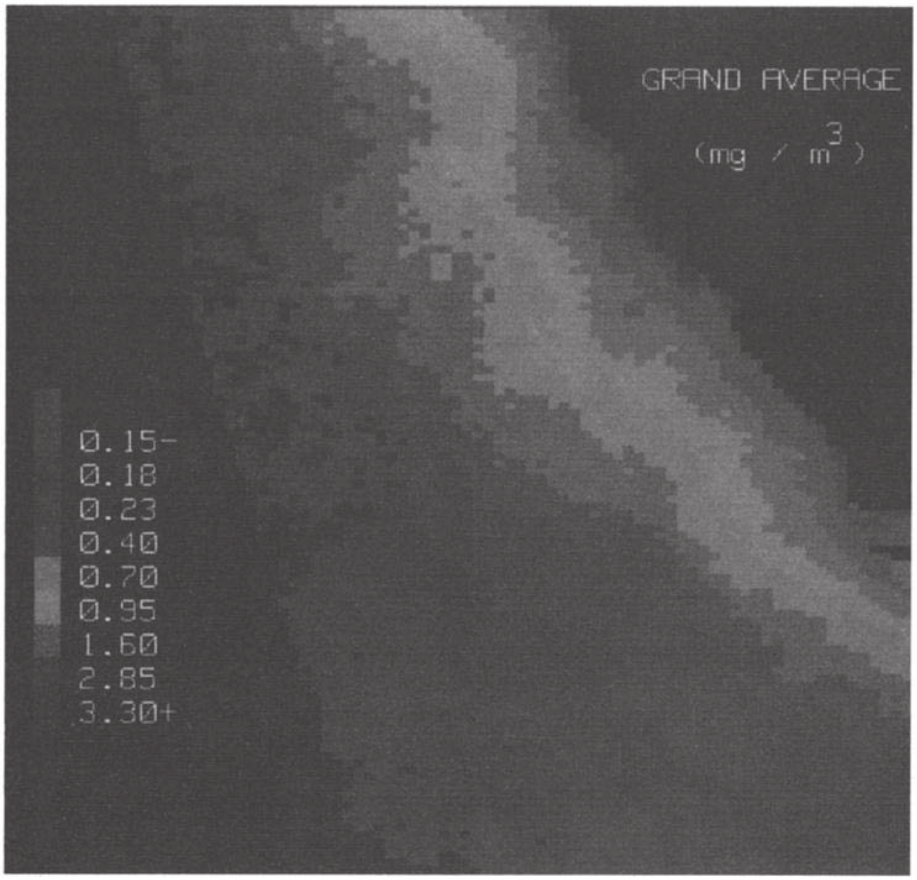

Plate 1*e*

Plate 1 (continued)

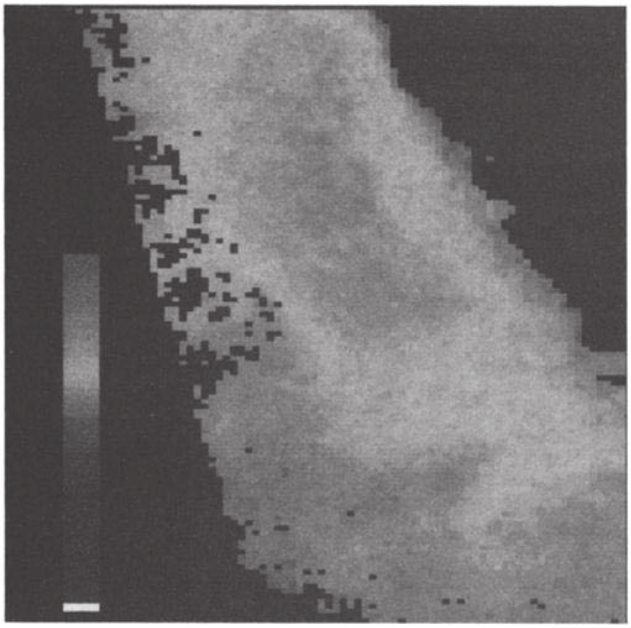

Plate 2*a*

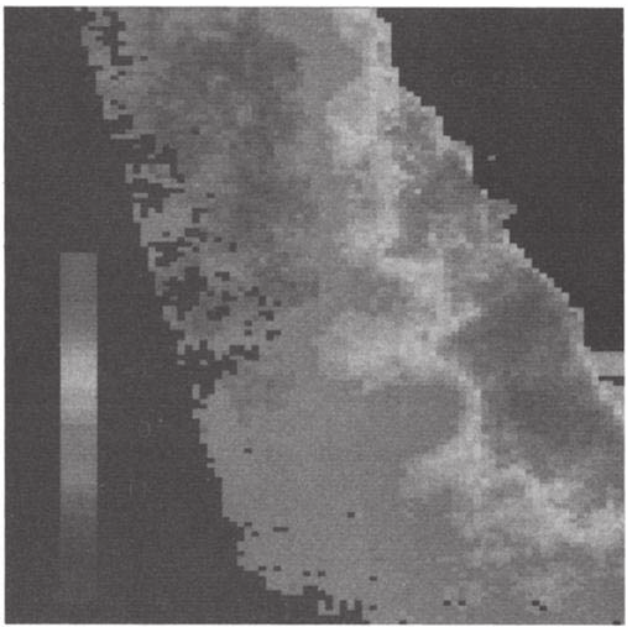

Plate 2*b*

Plate 2. (*a*) First EOF mode for phytoplankton pigment. (*b*) Second EOF mode for phytoplankton pigment. (The color version of this figure can be found in the separate color section in this issue.)

coefficients 50 km wide near the coast with a broad region of small, negative coefficients in the southwest corner of the study domain. This pattern is similar to the long-term spring–summer distribution of zooplankton displacement volume as measured by CalCOFI [*Chelton*, 1982; *Chelton et al.*, 1982].

The amplitude time series of this mode (Figure 2*a*) will be described for three different time periods: spring (March–May), late spring–early summer (June–July), and late summer–early fall (August–October). In spring, the amplitudes drop to negative values in March–April (around year days 80 and 450) in 1980 and 1981. Although this drop is more pronounced in 1980, it is more persistent in 1981. The combination of the mode with the negative amplitude corresponds to a strong increase in pigment in the offshore domain (Figure 2*a*) compared with the average (Plate 1*e*). A similar drop in the amplitude occurs in 1982 (around day 840), though it is barely detectable. No such drop is visible in 1983.

After the spring episode, the amplitudes recover in late spring–early summer 1980 and 1981, recrossing zero around late April (day 120) in 1980 and mid-May in 1981 (day 510). The

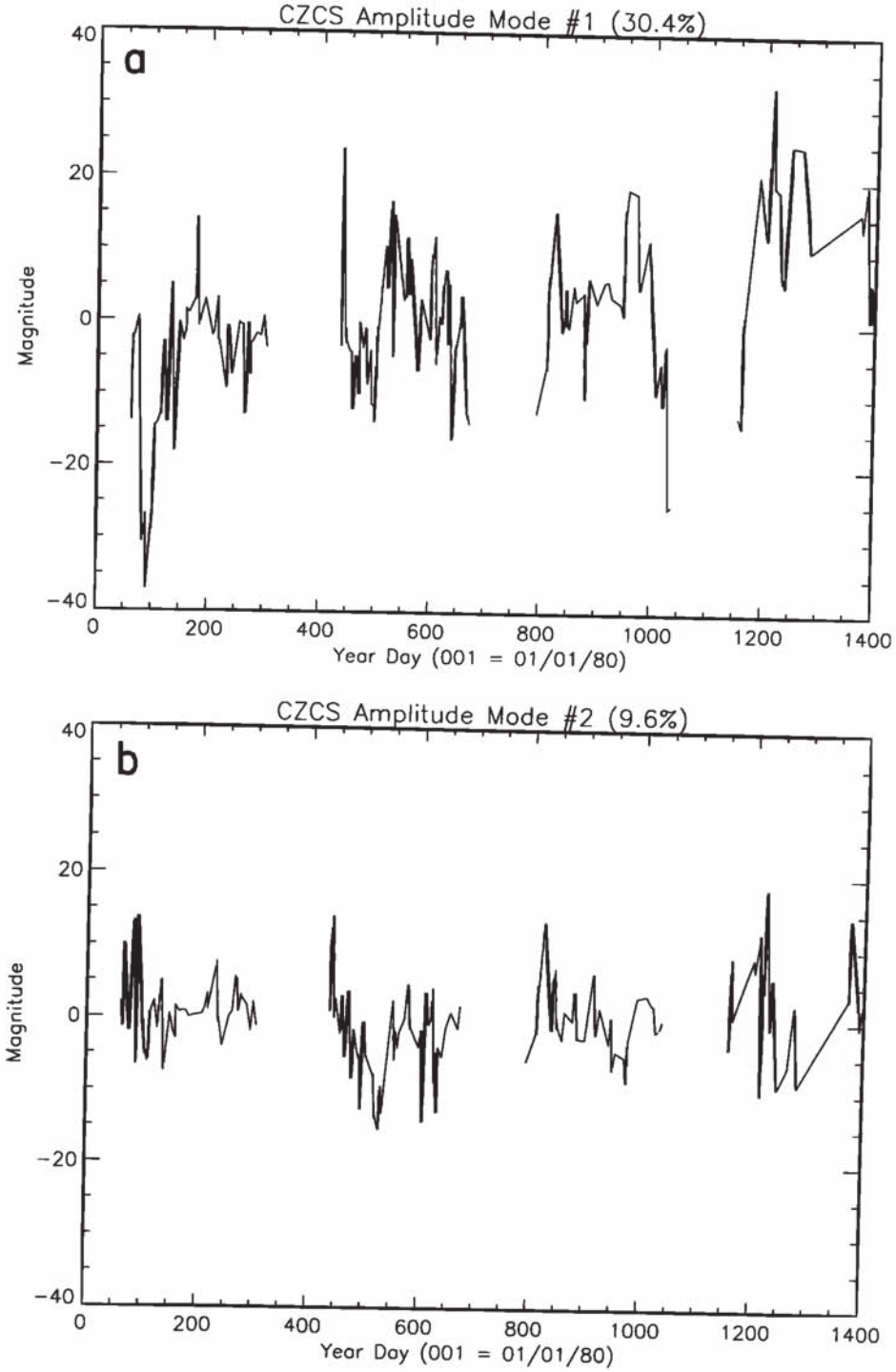

Fig. 2. (*a*) Amplitude time series for the first pigment EOF mode. (*b*) Same as Figure 2*a* but for second EOF mode.

amplitudes oscillate around zero during early summer in 1980, whereas the amplitudes become strongly positive in 1981. In 1982, the first mode is near zero for most of the spring–early summer and were generally positive during this period in 1983.

The transition to the late summer–early autumn period in 1980 occurred in mid-August (day 210) as the amplitudes become generally negative. In 1981, the amplitudes oscillate around zero after mid-August (day 590). There are some large negative values around day 610 (mid-September). In 1982, the amplitudes become strongly positive in early August (around day 930). A sharp drop occurs near day 990 in 1982 (late September), similar to 1981. This episode may be a "fall transition" that has been described by *Thomas and Strub* [1990], analogous to the spring transition. It seems to have been more pronounced in 1982 than other years. In 1983, the first mode amplitudes remain generally positive, with a sharp drop in early October.

The second mode (Plate 2*b*) accounts for 9.6% of the variance and consists of a scalloped, broad band of negative coefficients near the coast. This band broadens from Point Arena to Point Conception. Offshore, the coefficients are positive, especially in the northern part of the domain. The offshore scallops tend to be associated with the coastal headlands of Point Reyes, Point Sur, and Point Conception.

The amplitude time series (Figure 2*b*) starts out positive in all 4 years. In 1980, it is generally negative from about late May (day 150) through June (day 180). The spring–early summer pattern in 1981 is similar except that the amplitudes become strongly negative around day 460 (mid-April), reaching a maximum around day 530 (mid-June). The pattern in 1982 resembles that from 1980 although the period after day 850 (late April) has less intense negative values. The spring–early summer time period in 1983 from March through May (days 1160–1250) is strongly positive compared with the previous 3 years. There are two negative episodes in June 1983. For the summer–early fall period, the amplitudes generally oscillate around zero in 1980, 1981, and 1982. There are isolated negative events in late August–early September in all 3 years (days 250, 600, 630, and 950). These negative events were more persistent in 1982 between days 950 and 980. No such episodes were observed in 1983 although the sampling was much less in 1983 than other years. As with the first mode, the general pattern of the time amplitudes is similar for all 4 years; the amplitudes become negative about 30–50 days after the spring transition with the longest lag occurring in 1983. The amplitudes oscillate around zero through most of the summer except for some episodes of negative values in September.

The fact that the first two modes account for only 40% of the total variance is not surprising given the poor sampling available with the CZCS data. The low variance implies that there is considerable unresolved mesoscale variability in the data set.

In addition to calculating the EOFs for the 4-year time series, we also calculated them for each year separately. Obviously, one would expect the EOFs to differ simply because the means are different for the 4 years (Plate 1). The first mode for all 4 years was essentially the same. The southward extent of the broad "tongue" of large, negative coefficients varied between the years. In 1981, the tongue was deflected to the west and did not extend past Point Conception as in the overall mode 1 (Plate 2*a*). In 1983, the tongue began to break up just north of Point Conception. The second and third modes varied considerably between the 4 years. One would expect most of the differences to appear in the higher modes. In 1981, the filamentous region of negative coefficients was much more intense and extended farther offshore. This likely resulted in the apparent deflection of the first mode offshore in 1981. The second mode was less coherent in 1980, and on the basis of examination of both the modes and the amplitudes, the second and third modes were switched in terms of their contribution to the total variance in 1982 and 1983. Table 1 shows the distribution of variance among the three modes for all 4 years. Much of the change in the percentage of variance is likely a result of changes in the amount of sampling. That is, 1982 and 1983 were sampled less often than 1980 and 1981. Thus we consider only the relative placement of the modes to be significant. That the second mode (the "scalloped" mode) became the third mode in both 1982 and 1983 attests to its lesser importance in those years.

TABLE 1. Percentage of Total Variance in the First Three Modes of the CZCS Time Series

	1980	1981	1982	1983	All Years
Mode 1	27.2	23.3	34.3	31.1	30.4
Mode 2	10.3	12.5	10.4	19.7	9.6
Mode 3	4.9	7.3	7.1	8.9	4.7

For every CZCS image in the 4-year time series, we calculated the length of the identifiable filaments from Punta Eugenia, Baja California, to Vancouver Island, British Columbia. The length was estimated by measuring the farthest offshore extent of the high-pigment water and following the main axis of the filament back to shore. Thus the lengths do not take into account the meandering that may occur along a filament. These lengths also do not necessarily represent an actual flow pattern, which is likely to be more complex and involve onshore as well as offshore flow [e.g., *Strub et al.*, this issue; *Kosro et al.*, this issue]. However, this metric does give an indication of the offshore extent of the filaments. As a single filament often persisted over many images, we averaged these lengths into monthly bins covering roughly a 5° latitude region of the coast.

Figure 3*a* shows the average filament length for the period March–October from roughly Point Arena to Monterey. Figure 3*b* is the same except that it covers the region from Monterey to Point Conception. For the northern portion (Figure 3*a*), filaments are approximately 600 km long in spring, become shorter until about June (approximately 200 km long), and then increase in length through the rest of the summer. This pattern holds in 1980, 1981, and 1982, although the filaments reach their minimum length in July in 1982. The progression in 1983 is quite different; filaments tended to remain short throughout the year (order of 100–150 km). In the southern portion (Figure 3*b*), the same general pattern holds as in the north. The pattern of filament lengths is similar to that observed in the second pigment mode (Figure 2*b*); the filaments decrease in length as the amplitude of the mode becomes more strongly negative and then increase in length as the amplitude becomes smaller and eventually crosses zero. The negative amplitudes that occasionally occur in September are not resolved in the monthly averaged lengths. This pattern is not apparent in 1983 when the second-mode amplitudes do not become negative until about June (Figure 2*b*). In comparison, filaments off Vancouver Island and Washington/Oregon were approximately 300 km long in September 1983, considerably longer than filaments to the south in our study domain.

The mean FNOC-derived wind stress fields for the period March–October are shown in Figure 4 for each of the 4 years as well as for the grand mean for all 4 years. In general, the

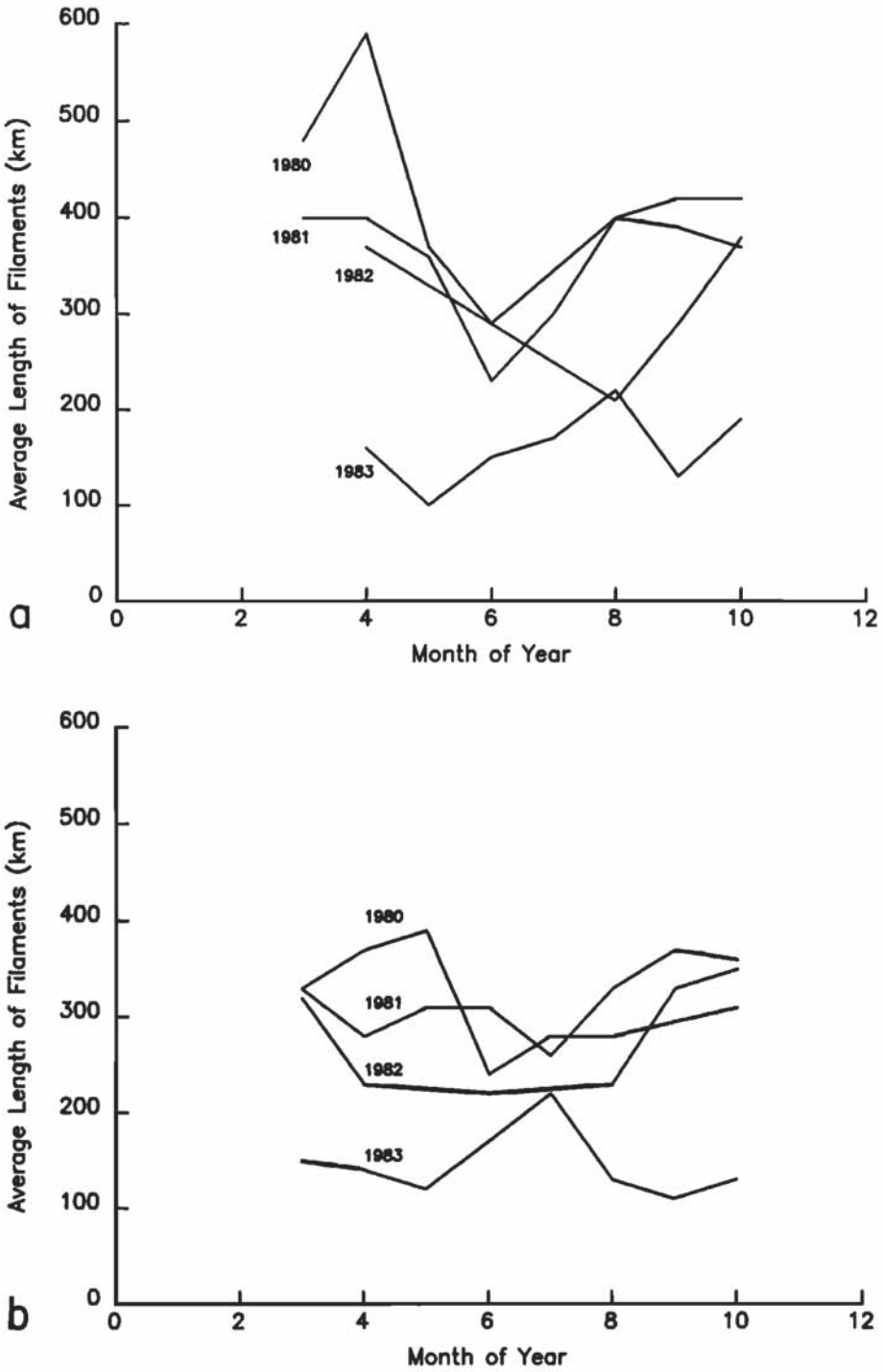

Fig. 3 (*a*) Average length of filaments on a monthly basis for the region between Cape Mendocino and Monterey. (*b*) Same as Figure 3*a* but for the region between Point Sur and Point Conception.

average wind stress is southward, similar to long-term averages derived from other data sets [e.g., *Hickey*, 1979; *Nelson*, 1977] for the spring–summer upwelling season. Maximum wind stress is offshore at approximately 236°E, leading to a positive curl in the wind stress field. *Strub and James* [1990] point out that the curl fields derived from analyzed fields such as LFM and FNOC data sets tend to underestimate the actual curl. The mean fields in 1980 and 1981 (Figures 4*a* and 4*b*) are essentially identical. The wind stress magnitudes were smaller in 1982 (Figure 4*c*), especially nearshore in the northern part of the domain. The mean field in 1983 is similar to the fields from 1980 and 1981 though slightly weaker (Figure 4*d*). The surprising point is that the mean field in 1983 is so similar to the other years. This has been noted by *Strub et al.* [1987]. The grand mean (Figure 4*e*) is similar to the means from 1980, 1981, and 1983.

The EOFs of the wind field were calculated using the full vector wind field, rather than by decomposing the field into its alongshore and cross-shore components. However, rather than show this mode and its corresponding phase and amplitude time series, we used a varimax rotation. The first varimax mode

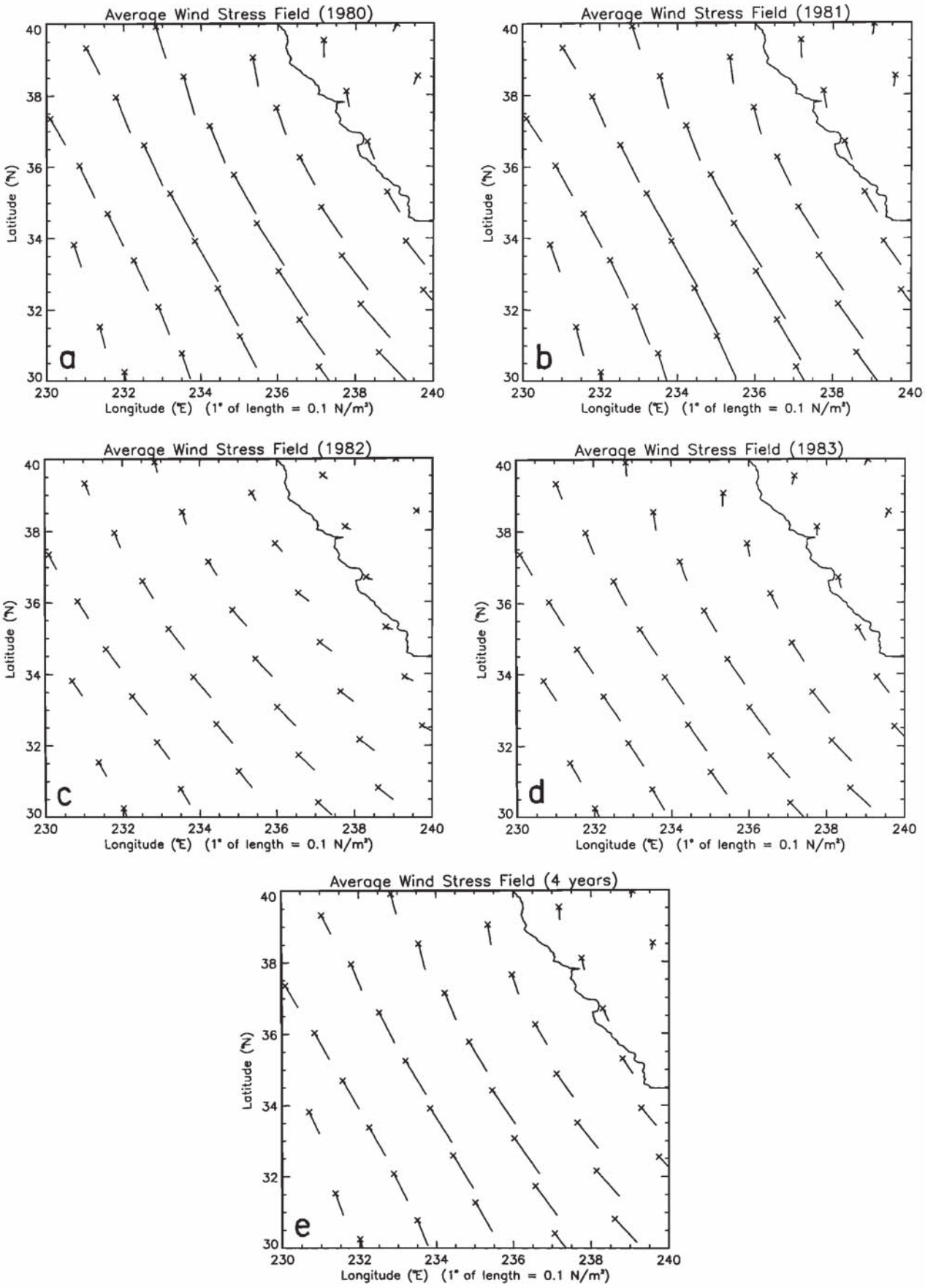

Fig. 4. (*a*) Average wind stress from FNOC for the period March–October 1980. (*b*) Same as in Figure 4*a* but for 1981. (*c*) Same as in Figure 4*a* but for 1982. (*d*) Same as in Figure 4*a* but for 1983. (*e*) Same as in Figure 4*a* but for all 4 years.

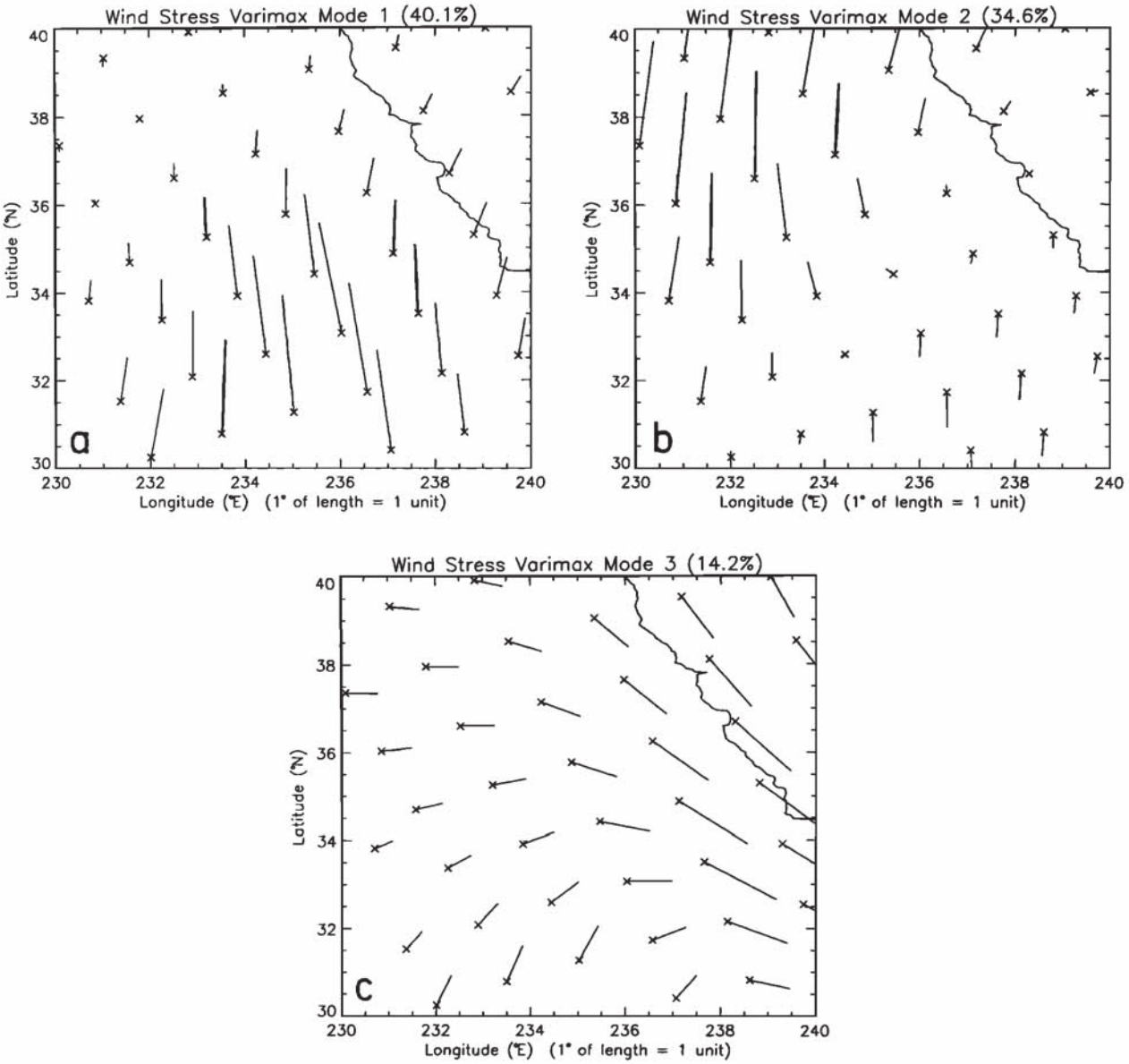

Fig. 5. (*a*) First EOF mode for wind stress. (*b*) Second EOF mode for wind stress. (*c*) Third EOF mode for wind stress.

(40% of the variance) is shown in Figure 5*a* and indicates a strengthening of the alongshore wind stress, primarily in the south central part of the study area. The amplitude time series for this mode (Figure 6*a*) generally starts out positive in March, becomes increasingly negative through midsummer, and then fluctuates near zero for the remainder of the upwelling season.

There is considerable interannual variability in this pattern. In 1980, a strong negative amplitude event around day 80 (late March) is apparent (corresponding to a southward wind stress fluctuation) which is most likely associated with the spring transition [*Strub et al.*, 1987; *Thomas and Strub*, 1990]. This event does not persist for long before the first mode enters a period of alternating southward and northward wind stress fluctuations of decreasing intensity through the spring–early summer period (days 100–180). The largest amplitude events in the first-mode amplitude are nearly always negative (southward fluctuations). In 1981, a similar spring transition event occurs in the first mode around day 450. In contrast with 1980, the following period contains more persistent, stronger southward fluctuations throughout the spring–early summer period (days 450–550). The spring transition in 1982 is far weaker and appears around day 840. Prior to this, the strong events are associated with northward winds (positive amplitudes). The subsequent spring–early summer period (days 850–940) has fewer strong southward episodes and has some relatively strong northward episodes. Although the spring transition occurred around day 1190 in 1983, the rest of the spring was dominated by strong, northward fluctuations. Strong southward episodes did not appear until about day 1225 (late May).

The late summer–fall period (days 180–300 in 1980, days 550–670 in 1981, days 940–1040 in 1982, and days 1300–1400 in 1983) also differed between the 4 years. In 1980, there was a roughly 30-day period where the wind fluctuations were fairly steady from the north (days 180–210). This was followed by a period of relatively small fluctuations of variable direction. This period ended in October as the first winter storms moved through, characterized by strong northward winds. In 1981, this

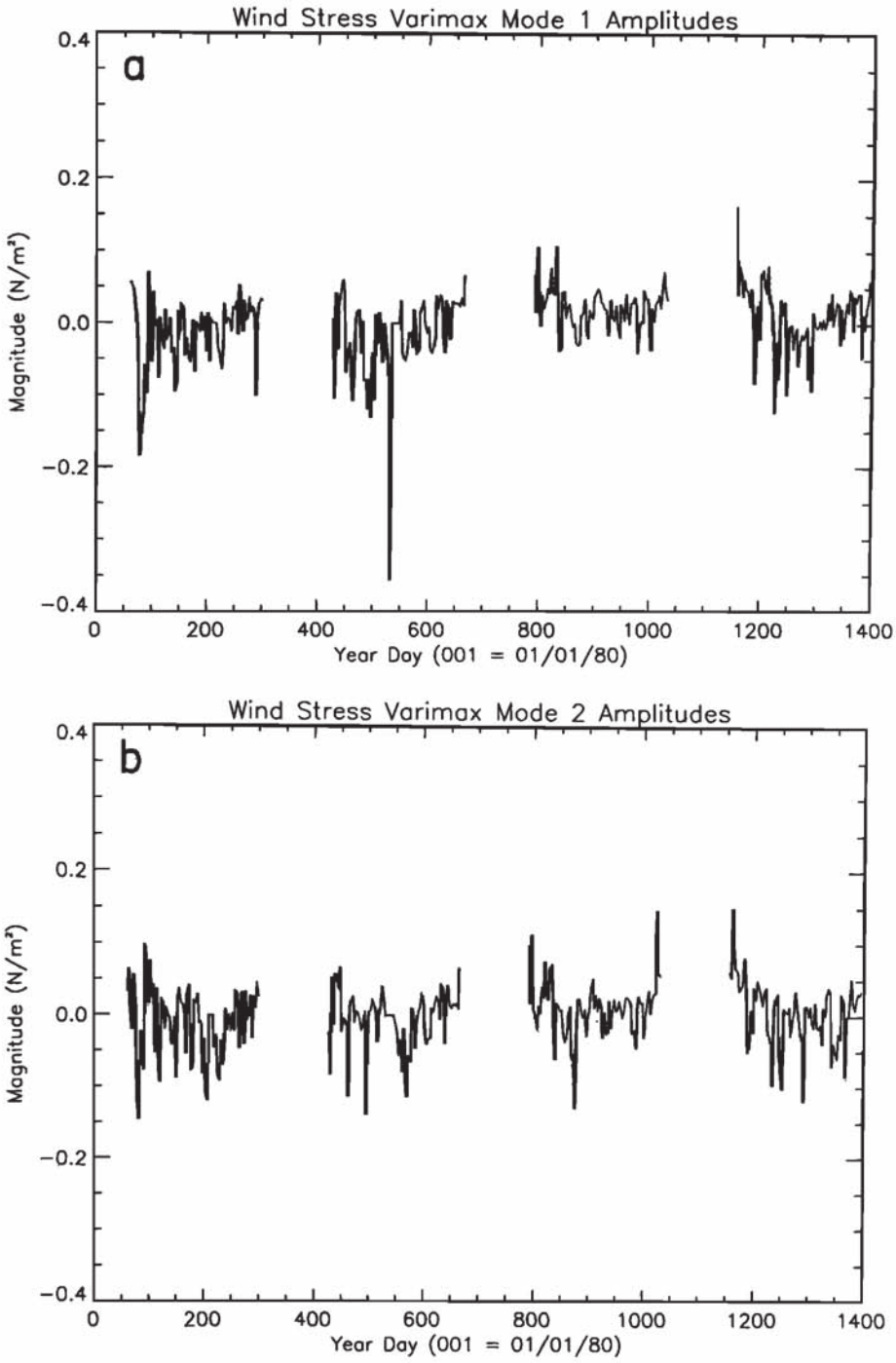

Fig. 6. (*a*) Amplitude time series for first wind stress mode. (*b*) Amplitude time series for second wind stress mode. (*c*) Amplitude time series for third wind stress mode.

period also was characterized by small fluctuations although they were more variable. Late summer–early fall in 1982 experienced generally weak fluctuations that were predominantly northward. A strong northward episode occurred in mid-October. Southward fluctuations persisted later into summer in 1983 and were followed by a period of weaker variability. During early autumn, there were increasingly strong events of northward fluctuations.

The second mode accounted for 34.6% of the variance and is shown in Figures 5*b* and 6*b* along with the corresponding amplitude time series. This mode represents a strengthening of fluctuations in the alongshore winds in the northwestern sector of the study area (Figure 5*b*). Note that there is a change in the direction of the fluctuation vectors along a line extending southwestward from the coast at about Point Reyes. As with the second mode, there is considerable variability in the sign of the amplitudes, as the wind stress fluctuations reverse in response to the propagation of disturbances through the atmosphere. The general pattern is similar for all 4 years; amplitudes are positive in early spring, then show increasingly negative fluctuations through spring and summer, and finally decrease (or become positive)

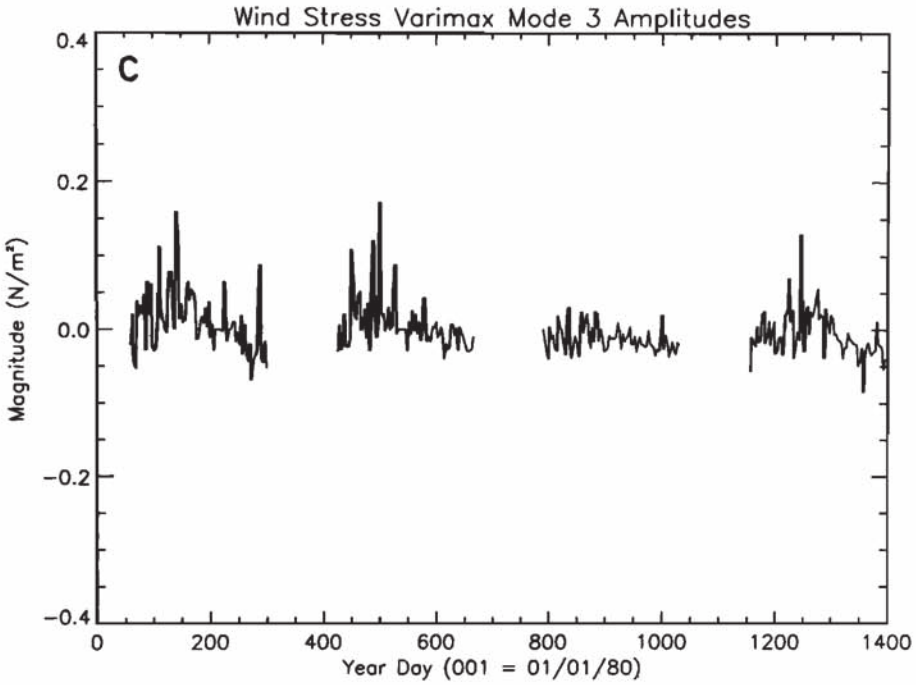

Fig. 6. (continued)

during late summer and early fall. These amplitudes are more variable in 1980 than in 1981, with larger positive fluctuations. In 1981, the fluctuations are smaller, except for a persistent period of negative values around day 590 (July). The amplitude time remains positive until later in spring 1982 (around day 850, in late April), but the negative fluctuations are smaller and less frequent than in the other 3 years. In 1983, the fluctuations remain strongly positive early in spring, with negative variations appearing around day 1250 (May).

The third mode and the associated amplitude time series are shown in Figures 5*c* and 6*c*. It accounts for 14% of the variance. The mode (Figure 5*c*) describes the decrease in wind stress in the offshore domain and a slight increase in the south portion near the coast. The fluctuations become alongshore near the coast. The general pattern of the amplitude time series (Figure 6*c*) is nearly a mirror image of the first mode (Figure 6*a*) with the amplitudes becoming larger in the positive sense, reaching a maximum in early summer. The amplitudes then decrease and fluctuate around zero for the remainder of the season. In this mode, 1980 and 1981 are relatively similar although the amplitudes are somewhat larger in spring–early summer in 1980. As with the first mode, the pattern in 1982 is much less intense than during the other 3 years. In 1983, the increase in the amplitudes occurred later in the year (around day 1225, corresponding to late June).

One of the consequences of the varimax method is that the time amplitudes are no longer uncorrelated as they are in conventional EOF analysis. We examined the correlation between the time amplitudes for these three wind stress modes as a function of season. As expected, some of the amplitudes are highly correlated. The first and second modes show the strongest positive correlation as the two modes represent variability in the alongshore wind stress (Figure 7*a*). We also plotted these amplitudes as a function of season and year (not shown). This positive correlation between the first and second wind mode amplitudes was noticeably weaker in 1981 during the late spring–early summer period. Figure 7*b* shows the scatter plot for the amplitudes of the first and third stress modes. There is a fairly high degree of negative correlation, and again the late spring–early summer period was conspicuously different in 1981 than in the other years. The relationship between the second and third mode amplitudes (Figure 7*c*) is more complicated. Although there is a general negative trend, there is considerably more scatter. The strength of the correlation was generally weaker in 1982 and 1983 in spring and early summer than in the other years, and the degree of correlation decreased beginning in late summer and was essentially absent by fall.

We also performed a complex EOF analysis of the wind stress vectors [*Hardy and Walton*, 1978]. The first mode of this analysis was similar to a combination of the first and second modes in the varimax analysis (Figures 5*a* and 5*b*) and corresponded to a uniform strengthening and weakening of the alongshore winds. The varimax procedure separates this into two modes, suggesting that there is alongshore variability in these fluctuations of the alongshore winds. The third mode in the complex analysis acted to increase or decrease the strength of the positive curl (present in the mean wind stress field), depending on the phase. In general, we saw a pattern where the curl was occasionally intensified and followed by relaxations, especially in spring–early summer and in particular in 1981. Periods of weaker curl intensification were more common in 1980 and 1982. This period of waxing and waning curl in spring–early summer was followed by a period of fairly steady, weak curl in summer in both 1980 and 1981. We reconstructed the wind stress fields from the first three complex EOF modes and amplitudes; these fields showed that curl was larger in 1981, especially in the area between about 32°N and 35°N and 236°E and 234°E.

We estimated the curl of the wind stress for both the LFM and the FNOC winds. The general patterns of the EOF modes and amplitudes for the two fields was similar, but the FNOC-derived curl field was noisier. The results of this analysis basically support those derived from the wind stress data; winds offshore in 1981 were stronger than average, resulting in a larger area of positive

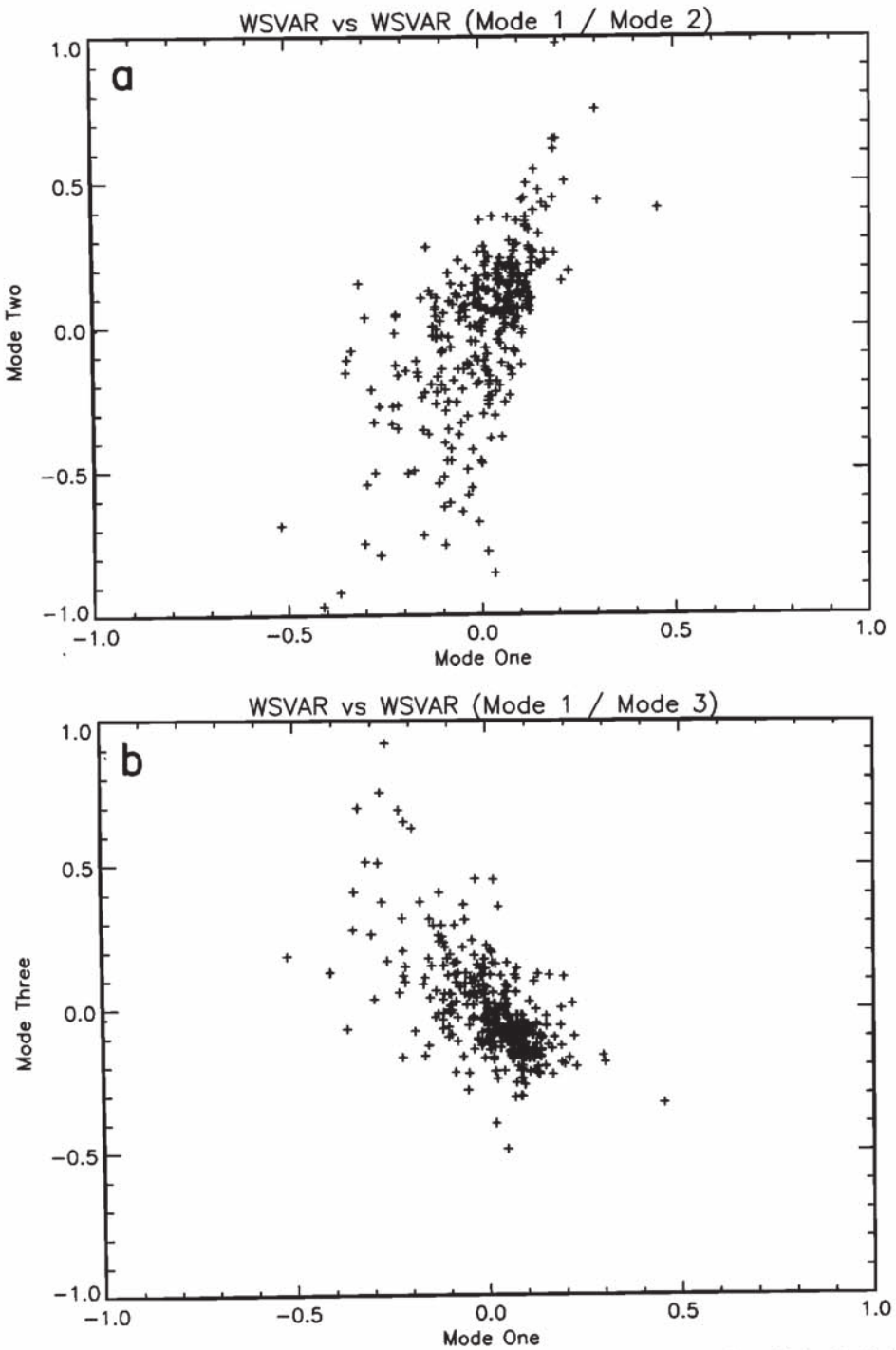

Fig. 7. (*a*) Scatter plot of amplitudes for first and second wind stress modes. (*b*) Scatter plot of amplitudes for first and third wind stress modes. (*c*) Scatter plot of amplitudes for second and third wind stress modes.

wind stress curl off central California. Although the strength of the curl was not that different, the spring–early summer period also had more strong positive curl events followed by relaxations.

DISCUSSION

CZCS Patterns

The first CZCS mode appears to be a "California Current/upwelling" mode that essentially describes the core of the California Current which is nearly uncoupled from the nearshore boundary. The timing of the spring drop in the amplitude of the first mode matches well with the date of the spring transition [*Huyer et al.*, 1979] as reported by *Thomas and Strub* [1989] (March 22, 1980, March 26, 1981, April 18, 1982, and April 4, 1983; corresponding to days 82, 451, 839, and 1190 in Figure 2*a*). The pattern of a broad bloom in the core of the California Current associated with the spring transition is consistent with the results of *Thomas and Strub* [1989]. The southward extent of this tongue of the California Current was less in 1983 and somewhat deflected offshore in 1981. In regards to interannual

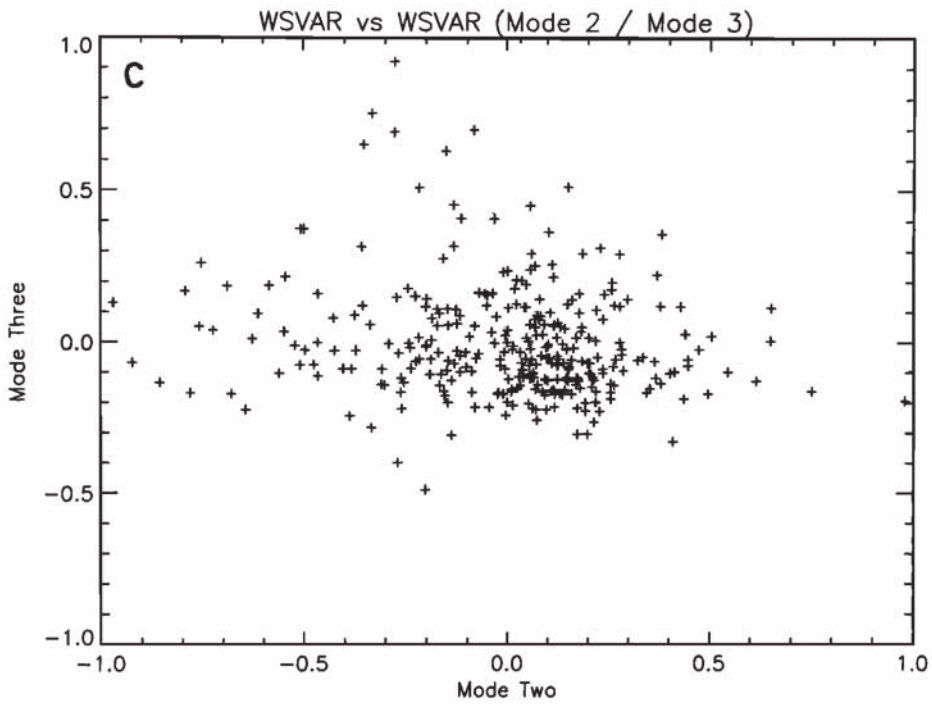

Fig. 7. (continued)

changes, Figure 2*a* shows that aside from changes in magnitude and timing, 1983 stands out as significantly different than the other years, although 1982 is perhaps intermediate. This is consistent with the pattern shown in the yearly means (Plate 1); pigment values in the main part of the California Current were generally much lower than average in 1983. However, if we account for the less frequent sampling in 1983, the years are not that different except for the spring period when amplitudes (days 1160–1250) were positive while the other years were negative (or near zero). This amplitude information, when coupled with the mode (Figure 3*a*), implies that concentrations were lower than average over the broad area of the California Current in spring 1983.

The second CZCS mode is a "filament" mode that describes the scalloped boundary between the offshore California Current and the nearshore, productive water. Its spatial pattern corresponds to some persistent features that have been observed in the California Current. *Simpson et al.* [1986] describe a recurrent eddy southwest of Point Conception that is visible as the region of positive coefficients between the westward and southwestward tongues of negative coefficients near Point Conception. *Brink et al.* [this issue] report on 2 years' worth of Lagrangian drifter observations. Many of the recurrent flow features traced by the drifter tracks coincide with the scallops in the second mode. This mode was stronger in 1981 than 1980 or 1982 and was absent until summer in 1983. The second mode also reflects the lengths of the filaments as determined from the original CZCS imagery. The pattern of filament lengths nearly mirrors the seasonal pattern of dynamic height [*Strub et al.*, this issue]; filaments are shortest when dynamic height variability is at its maximum.

The amplitude time series for the first and second modes generally move out of phase in spring–summer in 1980 and 1981 after the spring transition (Figures 2*a* and 2*b*); that is, maxima in the first mode generally correspond to minima in the second mode and vice versa. The opposite pattern prevails before the spring transition and in the September–October period. Note that the amplitudes generally move together throughout the spring in 1982 and 1983. Thus there is a spring bloom which affects most of the California Current, but as it deteriorates, the filaments begin to strengthen. The concentrations within the filaments increase while the actual lengths of the filaments decrease until about June, consistent with the overall decrease in pigment concentration in the main core of the California Current and slight decrease in pigment concentration nearshore as indicated in the first mode. This is also consistent with the pattern of filament length shown in Figure 3. These patterns are less obvious in 1982 and especially in 1983, when essentially the pretransition patterns prevailed until late May. After the filaments reach their maximum intensity (and shortest length) around June or July, they begin to "relax," lengthening and decreasing in pigment concentration. This pattern is occasionally interrupted by strong "filament" events in September. During this relaxation in August–September, filaments become apparent off the north coast of Washington and British Columbia. These filaments are much longer than those described by *Ikeda and Emery* [1984] (on the order of 200–300 km) and have the same appearance as those off the California coast. However, these filaments are not always associated with any obvious coastal topography such as headlands. In 1983 during the El Niño, filaments were fairly common off Washington and British Columbia whereas filaments were relatively uncommon and much shorter off California.

Wind Patterns

The first wind stress mode (using the varimax rotation) represents the strengthening and weakening of the alongshore winds over the southern portion of the study area (Figure 5*a*). Note that this mode has a maximum offshore at about 236°E so that negative amplitudes represent an increase in positive wind stress curl. The second mode (Figure 5*b*) is similar, but it represents changes in the alongshore wind stress in the northern portion and has a maximum at about 232°E. The third mode (Figure 5*c*) describes the variability in the cross-shore winds (especially in the offshore domain). Its increase nearshore in essence counteracts

the reduced winds present nearshore in both the mean wind stress (Figure 4*e*) and the other two modes.

The first and second modes are general highly correlated (in the positive sense), thus representing a uniform increase in the alongshore winds over the whole domain. The spring transition is particularly apparent in 1980 and 1981, appearing as a short, pronounced event in 1980 and as a long, less pronounced event in 1981. The other difference in the wind stress patterns between 1980 and 1981 was that the alongshore winds tended to remain highly correlated off northern and central California in 1980, whereas this correlation was much weaker in late spring and summer in 1981. This can be seen in Figures 6*a* and 6*b* (the first and second wind stress mode amplitudes) which indicate that the southward winds tended to be stronger in the southern portion during spring and early summer in 1981. Note that during this period the first and third (Figures 6*a* and 6*c*) modes were also uncorrelated in 1981, compared with 1980. The net result is that there was much stronger positive wind stress curl in 1981 than in 1980 in spring and early summer. This is consistent with the observations of *Halliwell and Allen* [1987]. In both years, there was a strong southward wind event in late July (days 200 and 590) in the northern sector (Figure 6*b*). This event was followed by increasingly weaker winds in both the northern and southern sectors.

The patterns of wind stress were much different in 1982 and 1983. Spring was dominated by northward events in both years with only a weak transition in 1982 and a much later transition in 1983. Of the 2 years, 1983 is the most similar to 1980 and 1981 after accounting for the delay in the onset of the southward (upwelling favorable) winds. The wind stress patterns in 1982 are unique in that southward winds are much weaker in the southern portion of the study area throughout the season (Figure 6*a*). In summary, wind stress becomes strong in the southward direction in the early spring over the entire study area. These winds eventually decrease beginning in midsummer. This decrease begins off central California, usually after a strong southward event off northern California. There is considerable interannual variability in this pattern; the spring transition often varies in strength, duration, and timing, and during some years in the region off central California, the southward winds increase without any parallel increase off northern California. This latter pattern results in strong positive wind stress curl off central California.

Comparison of CZCS and Wind Patterns

The obvious method of comparing EOF patterns is the use of canonical correlation analysis or principal estimator patterns [e.g., *Strub et al.*, 1990; *Davis*, 1977]. We attempted this technique with our data sets; because of the gaps and irregular sampling of the CZCS time series, none of the apparent relationships were significant. That is, the percent variance explained was always smaller than the artificial skill. Thus we are obligated to make only qualitative comparisons between the two data sets. A similar dilemma was faced by *Kelly* [1985] in analyzing satellite-derived SST images. The examination of these patterns requires either increased sampling or averaging so that only lower frequencies can be resolved, as was done by *Strub et al.* [1990].

We performed a regression analysis of the first CZCS mode and the wind stress modes as a function of year and season. During spring 1980 (defined as the period from March 1 to April 10), there was strong, positive correlation between amplitude time series of the first CZCS mode and the first wind stress mode and a slightly weaker correlation in 1981. The limited number of CZCS images in spring 1982 and 1983 make any interpretations problematic. This pattern continued into late spring (defined as April 10 to June 15) except that the correlation became negative in 1980 and the correlation was more strongly positive in 1981 and 1983. During the summer period (June 15 to August 31) and late summer (August 31 to October 31), there was no correlation in any year. A similar pattern prevailed in the relationship between the first CZCS mode and the second wind stress mode. It was positive in spring 1980 and 1981 and became negative in late spring 1980 while becoming more strongly positive in this period in 1981. This relationship remained positive in 1981, but by late summer there was essentially no correlation in any year. The relationship between the first CZCS mode and the third wind stress mode was similar. There was a negative correlation between the two fields in spring in 1980 and 1981 which vanished in late spring 1980 but remained through summer in 1981.

In spring, the first CZCS mode (Plate 2*a*) responds strongly to the onset of southward winds in 1980 and 1981 (positive correlation) as pigment concentrations increase in the core of the California Current. Presumably, phytoplankton are growing rapidly as a result of the input of nutrients into the euphotic zone, as described by *Thomas and Strub* [1989]. This "bloom" in pigment did not appear until late spring in 1983, as spring was dominated by northward winds. The combination of the three wind modes during the spring bloom phase suggest that the winds were relatively uniform over the entire study area with little curl.

In late spring, the relationship between the wind stress modes and the first CZCS mode becomes much weaker (negative or weak correlation) except in 1981. During this period in 1981, the southward winds remain strong off central California in the southern part of the study area and the first CZCS mode remains negative. In midsummer, there is a series of strong southward wind events in the northern sector in both 1980 and 1981, and there is little relationship between wind stress and the first CZCS mode after this period. Winds in 1982 were especially weak off central California, whereas they became stronger in 1983. The rapid weakening of the spring bloom in 1980 seems to be related to the decrease in southward winds in the region off central California. Similarly, the persistence of the bloom in 1981 appears to be related to the persistent upwelling-favorable winds off central California. The absence of a bloom in 1982 is related to the absence of southward winds, and the late bloom in 1983 is similarly related to the late arrival of these winds.

There is no apparent relationship between the first pigment mode and wind stress after summer. The coupling between wind forcing (as it affects nutrient supply to the euphotic zone) becomes much more complex than simply wind-driven upwelling. Depletion in the upper ocean and the subsequent deepening of the nutricline could result in the apparent lack of response of phytoplankton pigment concentrations to upwelling-favorable winds late in the season. We also note that the nearshore pigment values show little change as the offshore values increase, because of the small size of the mode coefficients nearshore (Plate 2*a*). This suggests that upwelling-favorable wind episodes are not closely coupled with pigment concentrations nearshore. Previous studies have shown that upwelling events may move high-pigment water offshore and replace it with lower pigment concentration water from depth [e.g., *Jones et al.*, 1988; *Abbott and Zion*, 1985]. Pigment sometimes increases nearshore during wind relaxations, perhaps a result of less intense mixing. Thus the relationship between phytoplankton concentrations and upwelling-favorable winds may be complex, both in time and space

The second CZCS mode (or filament mode) has a more complex relationship with wind forcing (Plate 2*b*). The zero crossing

in this mode roughly corresponds to a combination of the lines of maximum variability in the first and second wind modes (Figures 5*a* and 5*b*). As the area of negative coefficients in the second CZCS mode is roughly bounded by the boundaries in the wind stress fields, it appears that curl may play a role in the patterns of the filaments. The amplitude of the CZCS filament mode (Figure 2*b*) becomes more strongly negative after the spring transition in 1980 and 1981, reaching a maximum negative value roughly 30–50 days after the spring transition. In 1981, when this mode was at its strongest, several prominent events (Figure 2*b*) occurred in the late spring period (e.g., days 460, 490, and 520) and have corresponding events in the first and second wind modes (Figures 6*a* and 6*b*). Moreover, the dominance of the CZCS filament mode is matched by an equal dominance of the first wind stress mode in 1981, which corresponds to strong southward winds (and positive curl) in the domain off central California. In contrast, 1980 had a much weaker filament mode and winds were much more uniform in both the northern and southern domains. Also, the third wind stress mode was stronger in 1980 in the spring–summer period, corresponding to stronger winds nearshore and hence weaker positive curl. The weakening of the filaments which occurs in midsummer appears to be related to a rapid weakening of the southward winds in the southern sector off central California, as is shown in the first wind stress mode. Occasionally, the filament mode restrengthens in late summer, and this pattern seems to correspond to strong southward events off northern California, as is shown in the second wind stress mode (Figure 6*b*).

Similar comparisons can be made with the patterns in 1982 and 1983. The filament mode in 1982 was essentially absent (Figure 2*b*), and the first wind mode was only slightly negative (or even positive) for much of the year. A notable exception occurred late in the season around September (day 950) when the second CZCS mode became strongly negative and there were some fairly strong negative amplitudes in the first and second wind modes. In 1983, the onset of the filaments (characterized by negative amplitudes in the second CZCS mode) did not occur until much later than usual (around late June), which corresponds well with the onset of strong negative amplitudes in the first and second wind stress modes.

There is a general pattern of wind stress and the response of pigment patterns in the California Current. Prior to the spring transition, wind stress is dominated by strong northward episodes, and pigment is low and relatively uniform throughout the California Current domain. The first strong southward wind event soon results in a bloom of phytoplankton that is also uniformly distributed offshore. During the bloom, values nearshore tend to be slightly higher than average. After the spring transition, the phytoplankton pigment patterns do not retain a simple relationship with the strength of the southward wind stress. Rather, the patterns of wind stress curl appear to be more important. Depending on the variability and strength of these curl events, filaments begin to form at particular locations. The overall pigment concentration in the California Current drops as a larger fraction of the pigment is distributed within the filaments. The filaments also tend to become shorter during this period, which starts soon after the spring transition and usually reaches its maximum intensity in early summer. Wind stress (and curl) become much weaker and steadier in the mid-July to August period, and the filaments become much less prominent in terms of concentration although they increase in length. Isolated wind events occasionally reinvigorate the filaments. A final bloom in the fall occasionally appears with spatial structure similar to the spring bloom.

Several factors can alter this pattern. The spring transition event can occur at different times as well as with varying strength. As was pointed out by *Thomas and Strub* [1989], such variability can affect the strength and persistence of the resulting phytoplankton bloom. Southward winds and the curl of the wind stress can be absent in some years such as 1982 or delayed as in 1983. In some years, curl can be especially strong off central California, resulting in the development of prominent filaments, as in 1981. Although such variability can confuse the interpretation of the data, in our opinion it actually the strengthens the notion that wind and pigment patterns in the California Current are coupled, albeit in a complicated manner. That is, a relatively coherent picture of wind and pigment can be put forth to explain the observed interannual changes.

Filaments in the California Current

We define the jet (or meander) as the narrow, high velocity region separating the cold, high-pigment inshore water from the warmer, low-pigment offshore water and the filament as the "tongue" that extends seaward between the offshore-flowing jet and the return flow [*Hood et al.*, this issue]. Filaments tend to recur at particular locations along the central California coast. This is consistent with the SST observations reported by *Kelly* [1985] for data from 1981 and with drifter observations by *Brink et al.* [this issue]. The filaments (or scallops) are present in the mean pigment field (Plate 1*e*) off Cape Mendocino, Point Arena, and Point Sur; filaments to the south of Point Sur appear in the second mode (Plate 2*b*). This suggests that during the spring–summer season (March–October) the filaments are a relatively persistent feature in the California Current, particularly in the northern part of the domain. The intensification of the filaments appears to be related to the strength and variability of the positive wind stress curl rather than solely to the strength of the upwelling-favorable winds. That is, both the seasonal and interannual patterns of the filament mode as well as its spatial pattern appear to be coupled with the patterns of the wind stress curl. For example, filaments were intense in the second CZCS mode when the first wind stress mode was especially strong, corresponding to strong positive curl in the area off central California. In 1980, filaments tended to be weaker in this region, corresponding to weaker wind stress curl. Filaments did not appear until midsummer in 1983, again consistent with the strengthening of curl. It is also interesting to note that the filaments reach their maximum intensity about 30–50 days after the positive curl is set up, which is the time scale proposed by *Chelton* [1982] for time-dependent Ekman pumping to develop in response to wind stress curl.

Chelton [1982] suggested that the Ekman pumping mechanism was responsible for the offshore maximum in zooplankton biomass as it would increase nutrient flux to the euphotic zone and hence increase primary and secondary production. *Chelton* [1982] based this hypothesis on the spatial correspondence of the curl and zooplankton fields and on the temporal correlation of the two fields. *Chelton* [1982] also noted the absence of a correlation between upwelling and zooplankton biomass. A similar pattern is noted here; upwelling-favorable winds affect a broad region of the California Current in some years immediately after the spring transition. This bloom persists only a short time, after which the strength of the upwelling-favorable winds and pigment concentration eventually become uncorrelated. The fact that both zooplankton biomass and the strength of the filaments are apparently related to positive curl in the wind stress suggests that the filaments may be the manifestation of the high phytoplankton biomass necessary to support the observed zooplankton biomass, as was first suggested by *Chelton* [1982]. Chelton argued that such filaments were sites

for upwelling through the action of wind stress curl, rather than transporting offshore material that had been upwelled near the coast.

The filaments have been speculated to be the result of a meandering jet that goes unstable off Cape Mendocino [*Haidvogel et al.*, this issue] where the instability is driven largely by changes in coastal topography. Transport of coastal water offshore by semipermanent eddies has also been proposed as the underlying mechanism [*Simpson et al.*, 1986; *Mooers and Robinson*, 1984]. Whatever the process, the flow acts to increase the areal extent of the high-pigment water by deforming the boundary between the low-pigment and high-pigment waters. It appears that the "basic" meandering of the jet is likely driven by some sort of dynamic instability that does not vary much from year to year. This is borne out by the presence of the scallops in the mean pigment field off northern California as well as in many of the CalCOFI fields [e.g., *Lynn and Simpson*, 1987; *Peláez and McGowan*, 1986]. Whether this instability is driven by topography or semipermanent eddies has yet to be determined. However, the results presented here suggest that the seasonal intensification and decay of the filaments, as well as their interannual variability, is closely related to the strength and variability of positive wind stress curl, particularly off central California. As the CZCS filament mode (as well as the lengths of the filaments) can change rapidly (order of weeks), it is unlikely that eddies or instabilities can be responsible for such changes. As Ekman pumping can act on such time scales, it is a likely candidate. It also appears that the mechanism of spatial variation in the strengthening and relaxation of wind stress may also be important [*Davis*, 1985; *Kelly*, 1985]. Lastly, it should be noted that filaments appear off the relatively smooth Washington/Oregon coast during August–September, when there is usually strong positive wind stress curl [*Chelton*, 1980]. Thus headlands are not essential for the formation of filaments.

The present data address only the filaments and not the jet separating the filament from the oceanic water; however, the seasonal progression of geostrophic velocities presented by *Lynn and Simpson* [1987] shows an intensification in early summer at the time of maximum filament development. These data are based on long-term averages, but they are consistent with the data presented here. The pattern of a large California Current core overlain by a fluctuating field of filaments is consistent with observations reported by *Peláez and McGowan* [1986] and *Lynn and Simpson* [1987]. The timing of the appearance of the filaments, their recurrence at particular locations, and occasional reappearance in September–October is similar to results reported by *Peláez and McGowan* [1986].

CONCLUSIONS

Because of the sparse sampling by the CZCS, any conclusions regarding specific events and short time scales must be made with caution. In particular, 1982 and 1983 were sampled less frequently than other years. Thus we focused on general patterns in the data sets, and in a sense we relied on circumstantial evidence, as direct observations of some the processes (such as upwelling) were not available. The scenario that we present attempts to form a consistent framework to explain our observations. Although interannual variability is often viewed as an obstacle in deciphering underlying relationships, we have attempted to exploit it by essentially using it as series of separate "experiments" to see if our scenario remains consistent with the observations. Unfortunately, we cannot use a rigorous statistical analysis such as that of *Strub et al.* [1990] or *Chelton et al.* [1982], but the consistency arguments do give a useful results, much as those presented by *Kelly* [1985].

We conclude that wind forcing, in particular the curl of the wind stress, plays an important role in the distribution of phytoplankton pigment in the California Current. The spring transition varies in timing and intensity from year to year but appears to be a recurrent feature associated with the rapid onset of upwelling-favorable winds. This variability is closely related to the pattern of variability in the alongshore winds. Although the underlying dynamics of the filaments may be dominated by processes other than forcing by wind stress curl (such as eddies or topographically induced instabilities), it appears that the temporal and spatial patterns of curl may force the variability of the pigment patterns and the filaments. In particular, the region off central California (south of Point Arena) has prominent filaments when there is strong, positive wind stress curl in that region. In many years, these winds are absent (such as 1982) or are weaker (such as 1980). The separation of the wind field into two domains (a northern California region and a central California region) has been noted in other studies of winds and currents [e.g., *Strub et al.* 1987; *Halliwell and Allen*, 1987]. The interaction between wind stress curl and the filaments may be through Ekman pumping, as was postulated by *Chelton* [1982] to explain the zooplankton biomass maximum that occurs offshore in the California Current.

Acknowledgments. We thank Ted Strub and Corinne James for graciously providing access to the FNOC and LFM winds as well as valuable advice. J. Richman, K. Denman, D. Chelton, G. Lagerloef, and two anonymous reviewers provided useful comments on various aspects of this work. This research was supported by grants from the Office of Naval Research and the National Aeronautics and Space Administration.

REFERENCES

Abbott, M. R., and P. M. Zion, Satellite observations of phytoplankton variability during an upwelling event, *Cont. Shelf. Res.*, *4*, 661–680, 1985.

Abbott, M. R., and P. M. Zion, Spatial and temporal variability of phytoplankton pigment off northern California during Coastal Ocean Dynamics Experiment 1, *J. Geophys. Res.*, *92*, 1745–1755, 1987.

Balch, W. M., M. R. Abbott, and R. W. Eppley, Remote sensing of primary production, 1, A comparison of empirical and semi-analytical algorithms, *Deep Sea Res.*, *36*, 281–295, 1989.

Beardsley, R. C., C. E. Dorman, C. A. Friehe, L. K. Rosenfeld, and C. D. Winant, Local atmospheric forcing during the Coastal Ocean Dynamics Experiment, 1, A description of the marine boundary layer and atmospheric conditions over a northern California upwelling region, *J. Geophys. Res.*, *92*, 1467–1487, 1987.

Bernstein, R. L., Eddy structure of the North Pacific Ocean, in *Eddies in Marine Science*, edited by A.R. Robinson, pp. 158–166, Springer-Verlag, New York, 1983.

Brink, K. H., R. C. Beardsley, P. P. Niiler, M. Abbott, A. Huyer, S. Ramp, T. Stanton, and D. Stuart, Statistical properties of near surface flow in the California coastal transition zone, *J. Geophys. Res.*, this issue.

Carder, K. L., R. G. Steward, G. R. Harvey, and P. B. Ortner, Marine humic and fulvic acids: Their effects on remote sensing of ocean chlorophyll, *Limnol. Oceanogr.*, *34*, 68–81, 1989.

Chelton, D. B., Low frequency sea level variability along the west coast of North America, Ph.D. thesis, 212pp. Univ. of Calif., San Diego, La Jolla, 1980.

Chelton, D. B., Large-scale response of the California Current to forcing by wind stress curl, *CalCOFI Rep. 23*, pp. 130–148, Calif. Coop. Fish. Invest., La Jolla, 1982.

Chelton, D. B., Seasonal variability of alongshore geostrophic velocity off central California, *J. Geophys. Res.*, *89*, 3473–3486, 1984.

Chelton, D. B., and R. E. Davis, Monthly mean sea level variability along

the west coast of North America, *J. Phys. Oceanogr.*, *12*, 757–784, 1982.

Chelton, D. B., and M. G. Schlax, Estimation of time-averages from irregularly spaced satellite observations: With application to coastal zone color scanner estimates of chlorophyll concentrations, *J. Geophys. Res.*, this issue

Chelton, D. B., P. A. Bernal, and J. A. McGowan, Large-scale interannual physical and biological interaction in the California Current, *J. Mar. Res.*, *40*, 1095–1125, 1982.

Coastal Transition Zone Group, The Coastal Transition Zone program, *Eos Trans. AGU*, *69*, 698–699, 1988.

Davis, R. E., Techniques for statistical analysis and prediction of geophysical fluid systems, *Geophys. Astrophys. Fluid Dyn.*, *8*, 245–277, 1977.

Davis, R. E., Drifter observations of coastal surface currents during Coastal Ocean Dynamics Experiment: The method and descriptive view, *J. Geophys. Res.*, *90*, 4741–4755, 1985.

Denman, K. L., and M. R. Abbott, Time evolution of surface chlorophyll patterns from cross-spectrum analysis of satellite color images, *J. Geophys. Res.*, *93*, 6789–6798, 1988.

Eckstein, B. A., and J. J. Simpson, Cloud screening coastal zone color scanner images using channel 5, *Int. J. Remote Sens., in press*, 1991*a*.

Eckstein, B. A., and J. J. Simpson, Aerosol and Rayleigh radiance contributions to coastal zone color scanner images, *Int. J. Remote Sens.*, *12*, 135–168, 1991*b*.

Eslinger, D. L., J. J. O'Brien, and R. L. Iverson, Empirical orthogonal function analysis of cloud-containing coastal zone color scanner images of northeastern North American coastal waters, *J. Geophys. Res.*, *94*, 10,884–10,890, 1989.

Feldman, G. C., N. Kuring, C. Ng, W. Esaias, C. R. McClain, J. Elrod, N. Maynard, D. Endres, R. Evans, J. Brown, S. Walsh, M. Carle, and G. Podesta, Ocean color: Availability of the global data set, *Eos Trans. AGU*, *70*, 634–641, 1989.

Fiedler, P. C., Satellite observations of the 1982–1983 El Niño along the U. S. Pacific coast, *Science*, *224*, 1251–1254, 1984.

Flament, P., L. Armi, and L. Washburn, The evolving structure of an upwelling filament, *J. Geophys. Res.*, *90*, 11,765–11,778, 1985.

Gordon, H. R., and D. J. Castaño, Coastal zone color scanner atmospheric correction algorithm: Multiple scattering effects, *Appl. Opt.*, *26*, 2111–2122, 1987.

Gordon, H. R., D. K. Clark, J. W. Brown, O. B. Brown, R. H. Evans, and W. W. Broenkow, Phytoplankton pigment concentrations in the Middle Atlantic Bight: Comparison between ship determinations and coastal zone color scanner estimates, *Appl. Opt.*, *22*, 20–36, 1983*a*.

Gordon, H. R., J. W. Brown, O. B. Brown, R. H. Evans, and D. K. Clark, Nimbus 7 CZCS: Reduction of its radiometric sensitivity with time, *Appl. Opt.*, *22*, 3929–3931, 1983*b*.

Gordon, H. R., J. W. Brown, and R. H. Evans, Exact Rayleigh scattering calculations for use with the Nimbus-7 coastal zone color scanner, *Appl. Opt.*, *27*, 862–871, 1988*a*.

Gordon, H. R., O. B. Brown, R. H. Evans, J. W. Brown, R. C. Smith, K. S. Baker, and D. K. Clark, A semianalytic radiance model of ocean color, *J. Geophys. Res.*, *93*, 10,909–10,924, 1988*b*.

Haidvogel, D. B., A. Beckmann, and K. S. Hedstrom, Dynamical simulations of filament formation and evolution in the coastal transition zone, *J. Geophys. Res.*, this issue.

Halliwell, G. R., Jr., and J. S. Allen, The large-scale coastal wind field along the west coast of North America, 1981–1982, *J. Geophys. Res.*, *92*, 1861–1884, 1987.

Hardy, D. M., and J. J. Walton, Principal component analysis of vector wind measurements, *J. Appl Meteorol.*, *17*, 1153–1162, 1978.

Hickey, B. M., The California Current system — Hypotheses and facts, *Prog. Oceanogr.*, *8*, 191–279, 1979.

Hood, R., M. R. Abbott, P. M. Kosro, and A. Huyer, Relationships between physical structure and biological pattern in the surface layer of a northern California upwelling system, *J. Geophys. Res.*, *95*, 18,081–18,094, 1990.

Hood, R., M. R. Abbott, and A. E. Huyer, Phytoplankton and photosynthetic light response in the coastal transition zone off northern California in June 1987, *J. Geophys. Res.*, this issue.

Huyer, A. E., Coastal upwelling in the California Current system, *Prog. Oceanogr.*, *12*, 259–284, 1983.

Huyer, A. E., E. J. Sobey, and R. L. Smith, The spring transition in currents over the Oregon continental shelf, *J. Geophys. Res.*, *84*, 6995–7011, 1979.

Ikeda, M., and W. J. Emery, Satellite observations and modeling of meanders in the California Current system off Oregon and northern California, *J. Phys. Oceanogr.*, *14*, 1434–1450, 1984.

Jones, B. H., L. P. Atkinson, D. Blasco, K. H. Brink, and S. L. Smith, The asymmetric distribution of chlorophyll associated with a coastal upwelling center, *Cont. Shelf Res.*, *8*, 1155–1170, 1988.

Kelly, K. A., The influence of winds and topography on the sea surface temperature patterns over the northern California slope, *J. Geophys. Res.*, *90*, 11,783–11,798, 1985.

Kosro, P. M., and A. Huyer, CTD and velocity surveys of seaward jets off northern California, July 1981 and 1982, *J. Geophys. Res.*, *91*, 7680–7690, 1986.

Kosro, P. M., A. Huyer, S. R. Ramp, R. L. Smith, F. P. Chavez, T. J. Cowles, M. R. Abbott, P. T. Strub, R. T. Barber, P. F. Jessen, and L. F. Small, The structure of the transition zone between coastal waters and the open ocean off northern California, winter and spring 1987, *J. Geophys. Res.*, this issue.

Large, W. G., and S. Pond, Open ocean momentum flux measurements in moderate and strong winds, *J. Phys. Oceanogr.*, *11*, 324–336, 1981.

Lynn, R. J., and J. J. Simpson, The California Current system: The seasonal variability of its physical characteristics, *J. Geophys. Res.*, *92*, 12,947–12,966, 1987.

Michaelsen, J., X. Zhang, and R. C. Smith, Variability of pigment biomass in the California Current system as determined by satellite imagery, 2, Temporal variability, *J. Geophys. Res.*, *93*, 10,883–10,896, 1988.

Mooers, C. N. K., and A. R. Robinson, Turbulent jets and eddies in the California Current and inferred cross-shore transports, *Science*, *223*, 51–53, 1984.

Mueller, J. L., Nimbus-7 CZCS: Confirmation of its radiometric sensitivity decay rate through 1982, *Appl. Opt.*, *24*, 1043–1047, 1985.

Mueller, J. L., Nimbus-7 CZCS: Electronic overshoot due to cloud reflectance, *Appl. Opt.*, *27*, 438–440, 1988.

Nelson, C. S., Wind stress and wind stress curl over the California Current, *NOAA Tech. Rep., NMFS-SSRF-714*, 1977.

Peacock, T. G., K. L. Carder, R. G. Steward, and C. O. Davis, Components of spectral attenuation for an offshore jet in the California Current coastal transition zone (abstract), *Eos Trans. AGU*, *69*, 1125, 1988.

Pearcy, W. J., and A. Schoener, Changes in the marine biota coincident with the 1982–1983 El Niño in the northeastern subarctic Pacific Ocean, *J. Geophys. Res.*, *92*, 14,417–14,428, 1987.

Peláez, J., and J. A. McGowan, Phytoplankton pigment patterns in the California Current as determined by satellite, *Limnol. Oceanogr.*, *31*, 927–950, 1986.

Preisendorfer, R. W., *Principal Component Analysis in Meteorology and Oceanography*, Elsevier, New York, 1988.

Richman, M. B., Obliquely rotated principal components: An improved meteorological map typing technique?, *J. Appl. Meteorol.*, *20*, 1145–1159, 1981.

Rienecker, M. M., and C. N. K. Mooers, Mesoscale eddies, jets, and fronts off Point Arena, California, July 1986, *J. Geophys. Res.*, *94*, 12,555–12,569, 1989.

Roesler, C. R., and D. B. Chelton, Zooplankton variability in the California Current, 1951–1982, *CalCOFI Rep. 28*, pp. 59–96, Calif. Coop. Fish. Invest., La Jolla, 1987.

Simon, R. L., The summertime stratus over the offshore waters of California, *Mon. Weather Rev.*, *105*, 1310–1314, 1977.

Simpson, J. J., C. J. Koblinsky, L. R. Haury, and T. D. Dickey, An offshore eddy in the California Current System, *Prog. Oceanogr.*, *13*, 1–111, 1984.

Simpson, J. J., C. J. Koblinsky, J. Peláez, L. R. Haury, and D. Wiesenhahn, Temperature–plant pigment–optical relations in a recurrent offshore mesoscale eddy near Point Conception, California, *J. Geophys. Res.*, *91*, 12,919–12,936, 1986.

Smith, R. C., X. Zhang, and J. Michaelsen, Variability of pigment biomass in the California Current system as determined by satellite imagery, 1, Spatial variability, *J. Geophys. Res.*, *93*, 10,863–10,882, 1988.

Strub, P. T., and C. James, Evaluation of surface wind fields over the coastal ocean off the western United States, in *Coastal Ocean Prediction Systems Workshop*, edited by C. N. K. Mooers, pp. 146–165, Joint Oceanographic Institutions, Washington, D. C., 1990.

Strub, P. T., J. S. Allen, A. Huyer, and R. L. Smith, Seasonal cycles of currents, temperatures, winds, and sea level over the northeast Pacific continental shelf: 35°N to 48°N, *J. Geophys. Res.*, *92*, 1507–1526, 1987.

Strub, P. T., C. James, A. C. Thomas, and M. R. Abbott, Seasonal and nonseasonal variability of satellite-derived surface pigment concentration in the California Current, *J. Geophys. Res.*, *95*, 11,501–11,530, 1990.

Strub, P. T., et al., The nature of the cold filaments in the California Current system, *J. Geophys. Res.*, this issue.

Thomas, A. C., and P. T. Strub, Interannual variability in phytoplankton pigment distributions during the spring transition along the west coast of North America, *J. Geophys. Res.*, *94*, 18,095–18,117, 1989.

Thomas, A. C., and P. T. Strub, Seasonal and interannual variability of pigment concentrations across a California Current frontal zone, *J. Geophys. Res.*, *95*, 13,023–13,042, 1990.

Willmott, A. J., Forced double Kelvin waves in a stratified ocean, *J. Mar. Res.*, *42*, 319–358, 1984.

Wooster, W. S., and J. L. Reid, Eastern boundary currents, in *The Sea*, vol. 2, edited by M. N. Hill, pp. 253–280, Interscience, New York, 1963.

M. R. Abbott and B. Barksdale, College of Oceanography, Oregon State University, Corvallis, OR 97331–5503.

(Received June 29, 1990;
accepted March 15, 1991.)

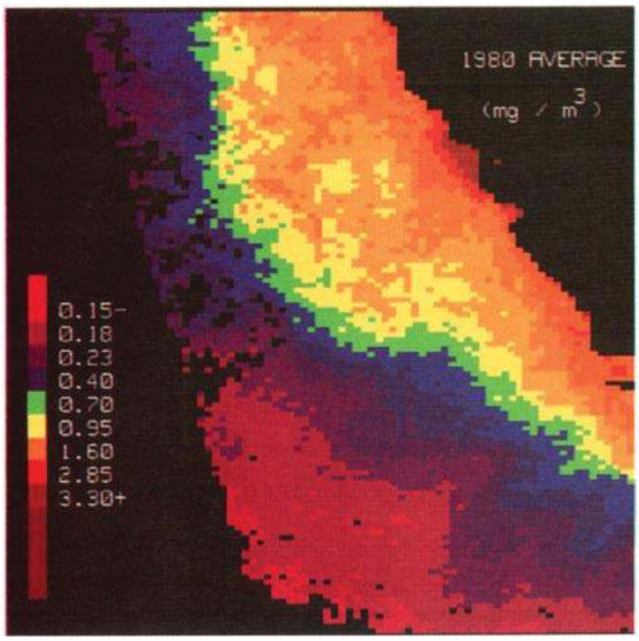

Plate 1*a*

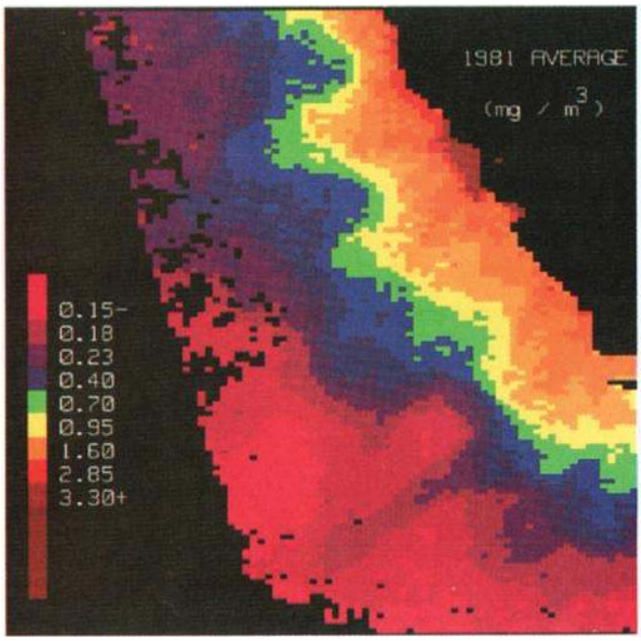

Plate 1*b*

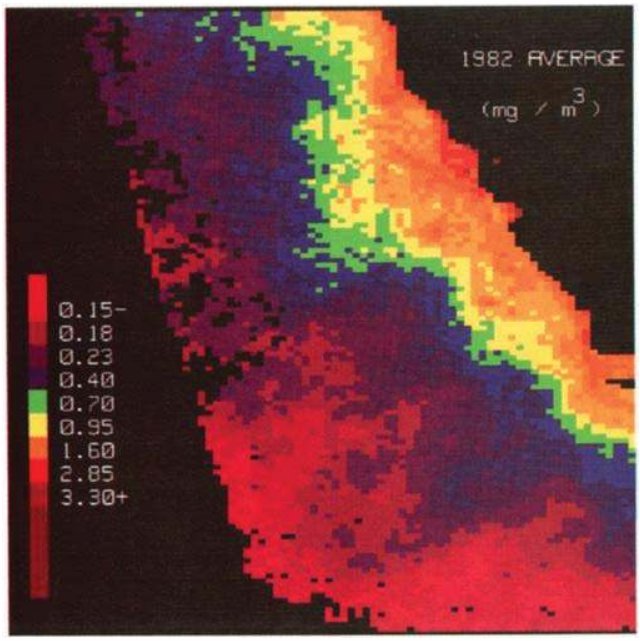

Plate 1*c*

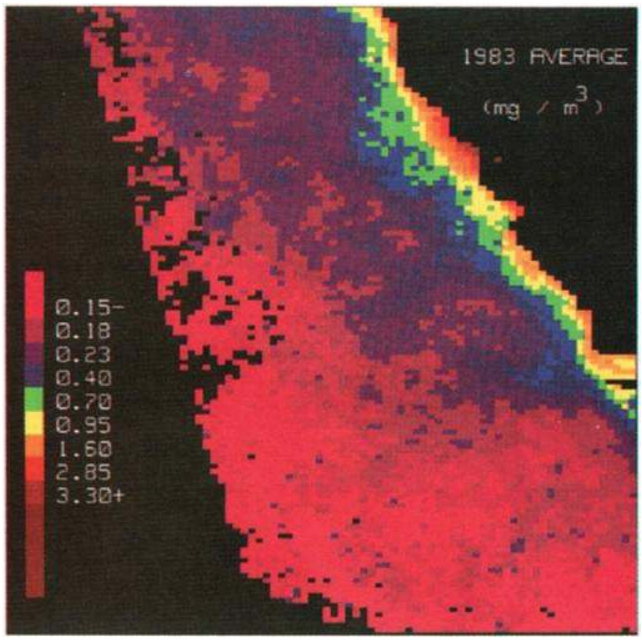

Plate 1*d*

Plate 1 [*Abbott and Barksdale*]. (*a*) Mean of CZCS-derived pigment images for the period March–October 1980. (*b*) Same as in Plate 1*a* but for 1981. (*c*) Same as in Plate 1*a* but for 1982. (*d*) Same as in Plate 1*a* but for 1983. (*e*) Same as in Plate 1*a* but for all 4 years.

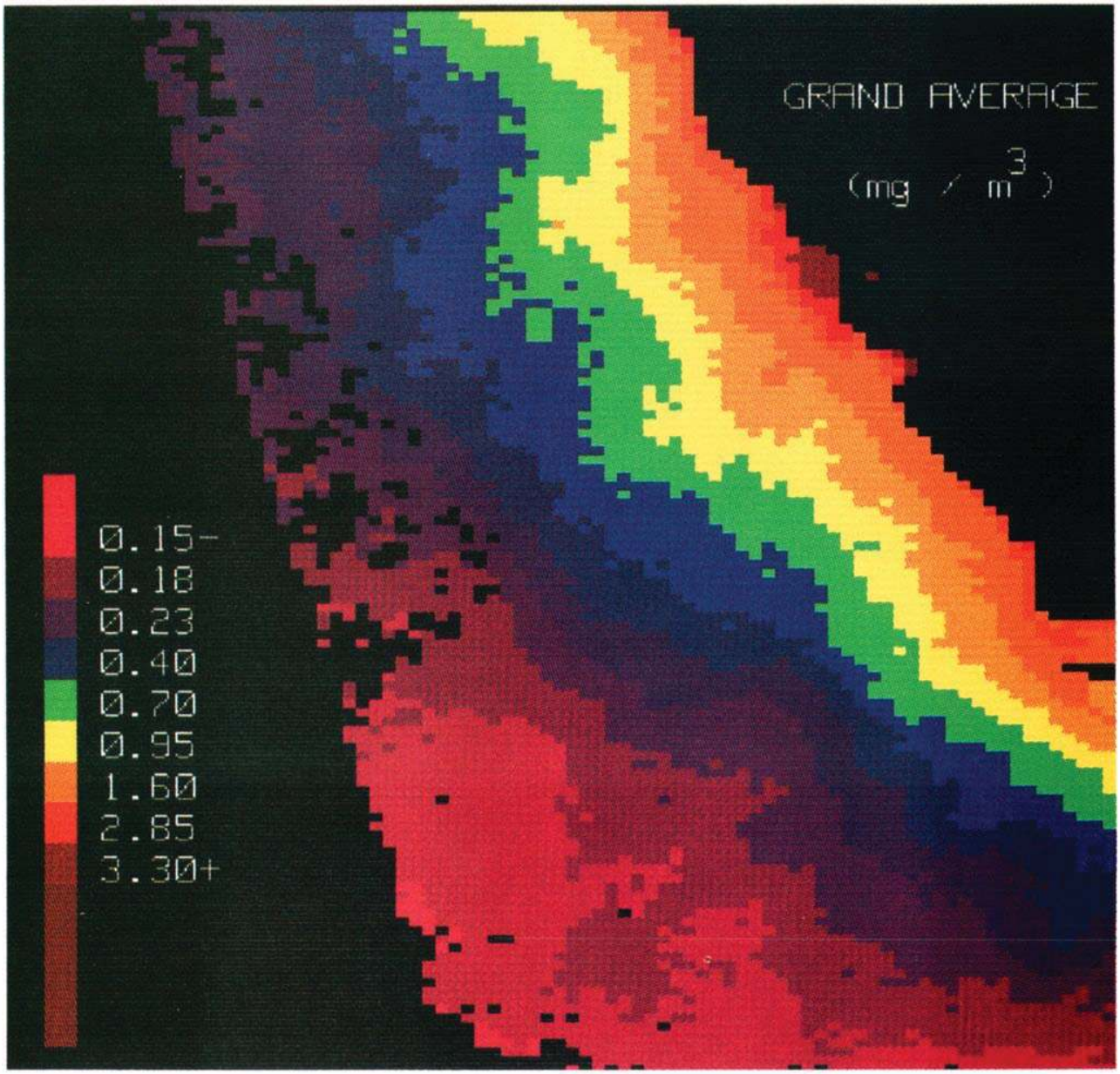

Plate 1*e*

Plate 1 [*Abbott and Barksdale*]. (continued)

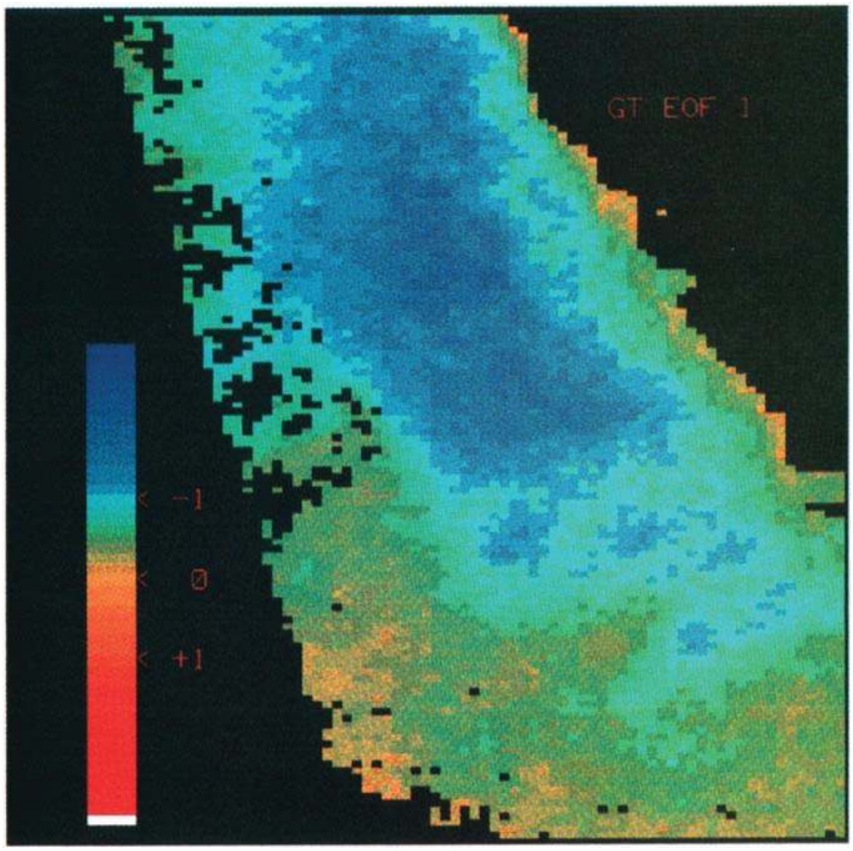

Plate 2*a*

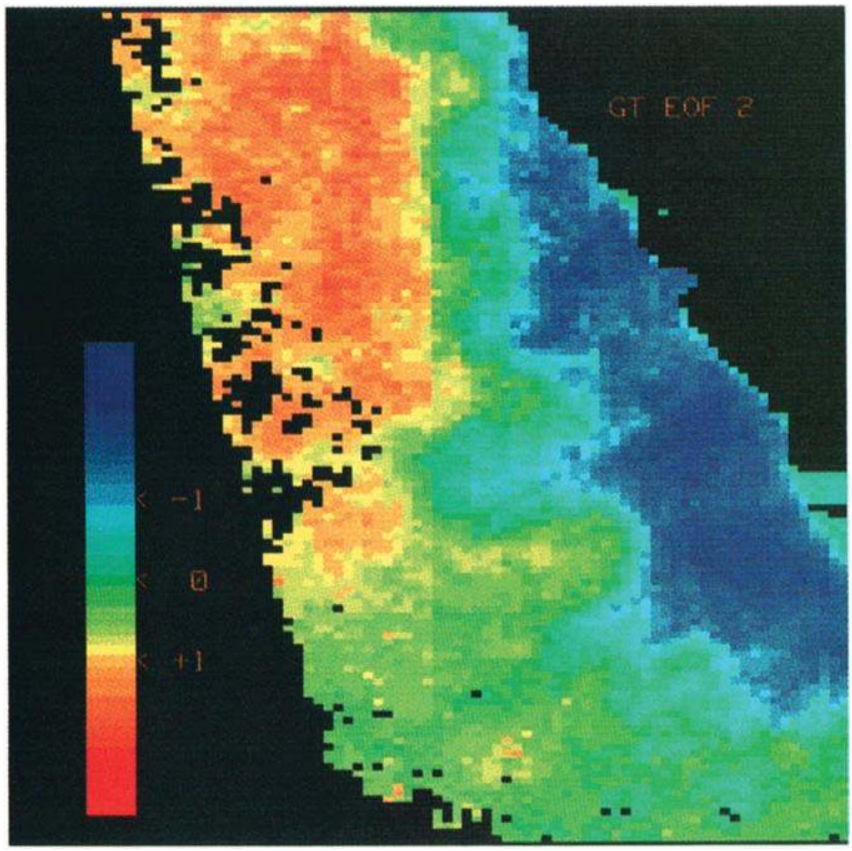

Plate 2*b*

Plate 2. ***[Abbott and Barksdale]***. (*a*) First EOF mode for phytoplankton pigment. (*b*) Second EOF mode for phytoplankton pigment.